Master Thesis For Automotive Engineering

Real Time SOC Estimation Based On EKF And UKF

Supervisor: Prof. Carabelli Stefano

Candidate: Xia Lei

July 2021

Abstract

"Safety, energy saving and environmental protection" is the eternal theme of automotive technology development. In today's global energy crisis and environmental problems are becoming increasingly serious, new energy vehicles, represented by electric vehicles, have become the future development trend of automobiles. As one of the key technologies of electric vehicles, the safe and efficient use of batteries depends on the accurate estimation of battery status. The state of the battery can be divided into two categories, one can be directly measured, such as voltage, current, temperature, etc. The other category cannot be directly measured, but can only be estimated by certain methods, such as the state of charge SOC, state of health SOH and so on. These state quantities are critical in the process of battery use.

There are many methods for estimating SOC, and most of them are based on the basic principle of ampere-time integration. Although the integration method is simple and easy to implement, there are two important problems: (1) the initial value of SOC cannot be estimated; (2) the inaccuracy of current measurement will cause cumulative errors. To solve these problems, the Kalman filtering method can be used. For our battery, we build two models, EKF and UKF, to predict its SOC variation and compare them respectively.

In this paper, the third-order Thevenin model was chosen to describe the dynamic behavior of the battery after comparing various equivalent circuit models and considering the accuracy and complexity of the model. The model is used to identify the parameters of the battery through pulse current charging and discharging tests. The results show that the Thevenin model can better describe the dynamic behavior of the battery, and its structure is simple and easy to identify the parameters. Then, the battery SOC is estimated based on the traceless Kalman filter (UKF) algorithm in Matlab environment. The accuracy and convergence speed of the algorithm are verified by artificially creating initial value errors and input noise by using WTP3 conditions to verify the effectiveness of the algorithm in a single working cycle. The simulation results show that the algorithm can gradually converge to the true value of SOC and follow it when the initial value is inaccurate and the input contains noise, and the estimation error does not exceed 4% in the middle and late stages of the working condition test.

Keywords: Electric Vehicle; State of Charge; Equivalent Circuit Model; Kalman Filter

Contents

CHAPTER 1

Introduction

1.1 Background and significance of the selected topic

Since the world's first car was introduced, after more than 100 years of development, the car has entered thousands of households, from a luxury product to a necessity in people's lives now. "Safety, energy saving and environmental protection" is the eternal theme of automobile technology development. Since the 21st century, with the rising oil prices and the aggravation of environmental pollution problems such as "haze", new energy vehicles represented by pure electric vehicles have gradually become the focus of attention in the industry by virtue of their energy-saving and environmental advantages.

At present, the research hotspots of new energy vehicles mainly focus on the three directions of pure electric vehicles, hybrid vehicles and fuel cell vehicles. As the core component of these three new energy vehicles, the development of battery technology is the key to the industrialization of new energy vehicles.

Although all major automakers are trying to promote new energy models, people's concern about the range of electric vehicles has hindered the promotion of pure electric vehicles, and the frequent incidents of spontaneous combustion of electric vehicles in recent years have made people pay extra attention to the safety of electric vehicles. For the power battery in electric vehicles, its safe and efficient use depends on the accurate estimation of the battery status.

The state of the battery can be divided into two categories, one can be directly measured, such as voltage, current, temperature, etc.; the other category can not be directly measured[1], but can only be estimated by certain methods, such as the state of charge (SOC) and the state of health (SOH) of the battery.

SOC is used to reflect the remaining capacity of the battery, which is related to the history of battery use. SOC is generally defined numerically as the ratio of the remaining capacity of the battery to its total dischargeable capacity, and is usually expressed as a percentage.

SOC is an important parameter in the course of battery use. The significance of SOC for a pure electric vehicle is similar to the fuel gauge on a traditional internal

combustion engine vehicle. Overcharging or over-discharging can cause irreversible damage to the battery, resulting in battery capacity decay, shortened life, and even danger[2].

On the other hand, for pure electric vehicles, an accurate display of the battery's SOC can help dispel the user's concerns about range.

Therefore, in order to fully utilize the performance of the battery and improve the safety of the battery, an accurate estimation of the SOC is required. However, unlike general electronic products, the operating conditions of automotive power batteries are very complex (large temperature range, high current fluctuation, frequent charging and discharging), resulting in strong nonlinearity of automotive power batteries, which makes it difficult to apply some previous SOC estimation algorithms to electric vehicles. Therefore, new SOC estimation algorithms for EV power batteries are being investigated.

SOH is used to represent the change in performance of a battery after a period of use compared to its initial performance. During use or storage, the battery will experience irreversible internal changes resulting in a decrease in capacity and an increase in internal resistance, resulting in a decrease in battery performance. This phenomenon is known as the aging of the battery. When the battery is aged, not only the performance deteriorates, but also the safety will deteriorate.

There is no uniform and precise definition of SOH. The SOH of a battery can be defined based on the changes of these performance parameters when considering different problems. When designing a Battery Management System (BMS), if the factors affecting the SOH and the variation of the SOH of the battery can be considered, it can help to estimate the SOC of the battery in each life stage more accurately, and then optimize the control strategy to prolong the life of the battery[3]. In addition, in recent years, the concept of automotive battery laddering has been proposed. Ladder utilization refers to the continued application of power batteries in other fields when their application in electric vehicles cannot meet the power and energy demand, so as to give full play to their application value and reduce the whole-life cycle cost of power batteries. If we want to realize the ladder utilization of batteries, it also depends on the accurate assessment of the relevant status of old batteries, especially the health status.

In conclusion, how to accurately estimate the non-directly observable state through the directly observable physical quantities in the battery is an important part of the battery application research work and a prerequisite to ensure the safe and efficient use of the battery.

1.2 Knowledge Base

1.2.1 Common SOC estimation methods

SOC is used to describe the remaining state of the battery. It is an abstract state concept, and cannot be measured directly like ordinary physical quantities, but can only be estimated by some methods. There are many methods to estimate the SOC, which can be roughly divided into two categories. The other type of methods need to use the battery model, use the pre-identified or trained model, and use the external parameters (such as voltage, current, temperature) of the battery as input to achieve the estimation of SOC according to certain algorithms[4]. The common SOC estimation methods are summarized below.

Discharge test method: the battery is subjected to a constant-current discharge test until it is emptied, and the integral of the discharge current over time is the remaining charge of the battery. Combined with the capacity information of the battery, the SOC of the battery is obtained. The discharge test method is accurate and reliable [3], it is applicable to all types of batteries and is commonly used for laboratory calibration. However, since discharge experiments take a lot of time and can only be performed offline, they are not applicable to running electric vehicles. In addition, the method is also not suitable for routine testing of electric vehicles because large depth discharges can significantly shorten the battery life.

Amperometric method: amperometric method is the most commonly used SOC estimation method. If the SOC of the initial state of the battery is SOC(0) , then the SOC of the battery at time t is :

$$SOC(t) = SOC(0) - \frac{1}{C_N}\int_0^t \eta(i(\tau))^i(\tau)d\tau \tag{1-1}$$

where C_N is the rated capacity of the battery; $i(\tau)$ is the current, which is usually specified as positive when discharging and negative when charging; $\eta(i(\tau))$ is the Coulomb efficiency, which is related to $i(\tau)$. The Coulomb efficiency of Li-ion batteries is generally very high, so it is often approximated as 1 in general studies. This equation is often used as the principle formula for other SOC estimation methods[5].

Although the ampere-time metering method is simple and easy to implement, there are three problems as follows.

(1) High requirements for current measurement accuracy, otherwise the inaccuracy of current measurement during long time use will cause cumulative errors.

(2) To consider the influence of battery charging and discharging efficiency, which is itself a difficult parameter to determine and requires a large amount of experimental data accumulation[6].

If the current can be accurately measured and the initial SOC can be accurately determined, then the ampere-time metering method can get good results.

Open-circuit voltage method: after a long enough period of resting, the open-circuit voltage of the battery (will be stable and approximately equal to the electric potential of the battery. However, this method requires the battery to be left for a long time (several hours), and is generally only applicable to the parked state, and can only provide the initial SOC value, but not continuously provide the SOC estimate. estimate. A simple SOC estimation method can be obtained by combining this method with the ampere-time integration method. However, since the discharge voltage plateau of Li-ion batteries is relatively flat, a small voltage measurement error may result in a large SOC estimation error, so the open circuit voltage method is not suitable for this type of battery system[7].

The load voltage method: under the constant load current, the polarization phenomenon inside the battery tends to be stable, and the variation law of the load voltage with SOC is similar to the variation law of the open circuit voltage OCV with SOC, so it can be used to estimate the SOC of the battery in real time. For electric vehicles, this method is not suitable for electric vehicles because of the large fluctuation of the load current during the actual application.

Internal resistance method: according to the different measurement methods, the internal resistance of the battery can be divided into two categories: AC impedance and DC internal resistance, and both of them are related to SOC. Some parameters in the AC impedance of the battery vary significantly with SOC and can be used to estimate the SOC in theory, but the AC impedance is affected by the experimental conditions, and the measurement requires specialized instruments and equipment, and sometimes the regularity of the parameter variation with SOC is not common, so it is seldom used for SOC estimation in real vehicles. The measurement result of DC internal resistance is affected by time, and the DC internal resistance of different types of batteries varies, so the application scope is also limited[8].

Kalman filter: the core idea of Kalman filter theory is to use the observed signal contaminated by noise to make an optimal estimate of the state of the dynamic system in the sense of minimum variance. The Kalman filter algorithm was earlier applied to

radar tracking, target navigation, and other fields. Since SOC is the state of a cell, the SOC estimation problem can be viewed as a state estimation problem in a noisy environment, and thus can be handled by Kalman filtering methods. Since 2002, Gregory L. Plett has published several papers on the estimation of SOC of Li-polymer batteries by Kalman filter method, which was introduced into the SOC estimation of Li-base batteries. In recent years, many researchers have used different battery models and different Kalman filter-derived methods for SOC estimation and obtained good results. Later, the dual Kalman filter method considering the battery aging process also appeared.

Compared with other SOC estimation methods, the Kalman filter method is more suitable for electric vehicle operating conditions where the current fluctuation is more drastic. By writing the SOC into the state variable, the Kalman filter method can give both the estimated value of SOC and the estimated error. In addition, the method can gradually converge to the true value, so it can overcome the problem of inaccurate initial estimation of SOC by the Anschluss method. However, the Kalman filter method also has some problems:

(1) the accuracy of the cell model and noise statistics seriously affects the accuracy of the calculation results, and an inaccurate model or noise statistics can easily cause the filtering instability or even divergence, which makes the algorithm lose its meaning;

(2) the convergence speed of the algorithm under large initial errors is slow

(3) The algorithm requires a large number of matrix operations, and if we want to improve the algorithm's ability to adapt to noise information, we need to integrate the adaptive algorithm, which will have a larger amount of operations and therefore the algorithm requires a higher computing speed of the processor[9].

The Kalman filtering algorithm will be described in detail in the subsequent sections.

1.2.2 Battery aging and health status

In the process of battery use, people want to know the SOH of the battery at any time, so that they can take timely measures to ensure the reliable operation of the battery. The SOH of the battery is related to various factors, such as temperature, charge/discharge multiplier, charge/discharge cut-off voltage, discharge depth, etc. Battery life refers to the battery in the process of use, the performance to meet certain

requirements of the use of time or use times. The research on battery life started in the early 1990s. Initially, it was mainly qualitative research, starting from the change of charge/discharge curve of lead-acid battery with the cycle of the battery to study the law of battery performance decay. The research on the life of nickel-based and lithium-based batteries started around 1995, and the applied methods were basically similar to those of lead-acid batteries. Around 1998, the concept of SOH was introduced in the research of lead-acid and nickel-hydrogen batteries. Since the emergence of lithium-ion batteries, people have gradually turned to the exploration of the aging mechanism of lithium-ion batteries, and many research results have emerged[10].

However, it can be seen from the previous studies that the performance degradation of Li-ion batteries is generally the result of a combination of factors. Starting from the essential causes of battery aging, Dr. Peng Bai from Tsinghua University has classified the causes of battery aging into three categories, i.e., stress effects, thermal mechanisms and chemical mechanisms. Peng Bai outlined the various factors affecting the use of batteries, the corresponding internal changes of batteries and the resulting aging failure modes.

The battery is defined as the starting point of its life when it leaves the factory, and reaches the end of its life when its performance no longer meets the needs. In actual use, the definition of the end of life of the battery varies according to the purpose of use. For applications requiring higher battery capacity, such as in pure electric vehicles, end-of-life is generally defined as when the battery capacity decays to 20% of the new battery capacity, i.e., when the usable capacity of the battery is 80% of the new battery. For such applications, when SOH estimation of batteries is performed, a capacity-based SOH definition is generally used, such as;

$$SOH = \frac{Q_{aged}}{Q_{new}} \tag{1-2}$$

where Q_{aged} is the nominal capacity of the current battery and Q_{new} is the nominal capacity of the new battery.

For convenience, SOH is generally defined between 0 and 100%, SOH of 100% means the battery is at the beginning of life, SOH of 0 means the battery reaches the end of life. A higher SOH indicates a longer usable life and more usable cycles[11]. Therefore, the SOH based on capacity decay has also been given as is defined as follows;

$$SOH = \frac{C - C_{EOL}}{C_{BOL} - C_{EOL}} \tag{1-3}$$

Where C is the current maximum available capacity of the battery, C_{EOL} is the maximum available capacity at the beginning of the battery life, and C_{BOL} is the maximum available capacity at the end of the battery life.

In some cases, even if the battery capacity decays to 80% of the initial capacity, the battery can still meet the usage requirements and continue to be used for some time. For example, in hybrid vehicles, batteries used as auxiliary power sources generally have high requirements for battery power and relatively low requirements for battery capacity. For this application, the end-of-life of the battery can also be defined from the perspective of power. When the battery power decay reaches a certain level, the battery life is considered to be over. Since the internal resistance of the battery directly affects the power characteristics of the battery, a definition of SOH based on internal resistance is generally used for SOH estimation of the battery, such as the definition proposed by Jonghoon Kim :

$$SOH = \left| \frac{R_{Diff}^{current} - R_{Diff}^{aged}}{R_{Diff}^{fresh} - R_{Diff}^{aged}} \right| \tag{1-4}$$

where $R_{Diff}^{current}$, R_{Diff}^{aged} and R_{Diff}^{fresh} are the diffuse internal resistance of the cell at the current, end-of-life and beginning-of-life times, respectively.

Electrochemical Impedance Spectroscopy (EIS) is a method that analyzes the AC impedance spectrum of a battery at different frequencies to understand the internal chemical state of the battery and to evaluate the external characteristics of the battery. The advantage of EIS is the high accuracy of the model, but the disadvantage is that the acquisition of internal battery parameters requires special equipment, which is expensive, and the process of parameter analysis is complicated. Matteo Galeotti et al. at the University of Rome II, Italy, used electrochemical impedance spectroscopy to establish the relationship between internal battery parameters and SOC by studying the variation of chemical substances in the battery with SOC, and to estimate the battery SOC based on the measured parameter variations. By studying and analyzing the electrochemical impedance spectroscopy, the changes in physical and chemical properties of the battery due to aging can also be obtained, i.e., the analysis of the

changes in capacity decay. Through the analysis of capacity decay change, the decay change of battery SOH can be obtained.

Artificial neural network method: Artificial neural network consists of a large number of interconnected neurons, each neuron observes the output of other neurons for calculation, and then chooses to trigger or not to trigger. Artificial neural networks help to learn automatically from a large amount of data by training the data with appropriate structures and samples. Researchers at the University of Illinois proposed a general data-driven approach that combines artificial neural networks with a double extended Kalman filter algorithm in order to eliminate the dependence of SOC and SOH estimation on the physical model of the battery. The artificial neural network is first trained offline to simulate the variation of the battery terminal voltage, and then the dual Kalman filter algorithm is used online to estimate the SOC and SOH of the battery.

1.3 The main content of this article

This paper takes the Samsung 50Ah battery pack as the research object and the PandaEV car as the battery operation carrier, and the core content is to design the real-time estimation algorithm of SOC and SOH of this battery pack during the operation of the car. The main part includes XXX chapters, and the content of each chapter is arranged as follows.

Chapter 1 introduces the important status and prospect of current new energy vehicles, briefly describes the current estimation methods and definitions of battery SOC and SOH, and presents the research content of this paper.

Chapter 2 introduces the basic parameters of the battery used in the experiment are introduced. The equivalent model of the third-order RC circuit used in our experiments is also selected. And the relevant parameters are fitted.

Chapter 3 describes the basic principles of the UKF EKF. Their recursive formulas are described. The theory and knowledge of UT transformations are introduced.

Chapter 4 designs a SIMULINK model for predicting SOC based on UKF and EKF, and integrates the module into our vehicle simulation model. The designed model performs the simulation task better with good accuracy and response speed.

Chapter 5 is a summary of the full work and an outlook on possible subsequent work.

CHAPTER 2

Battery model and its parameter identification

2.1 Selection of battery model

2.1.1 Classification of battery models

Building a battery model means to apply mathematical theory to describe the response characteristics and internal characteristics of the actual battery as comprehensively as possible. The response characteristics refer to the correspondence between the current and voltage of the battery; the internal characteristics refer to the relationship between the internal resistance, polarization voltage, temperature, SOC and other internal variables of the battery. If an accurate model of the battery is established, it means that the estimation of the internal state SOC of the battery can be achieved by applying relevant algorithms based on this model. At this stage of development, battery models can be divided into the following types according to the modeling mechanism: electrochemical mechanism model, equivalent circuit model, neural network model, etc.

The electrochemical mechanism model is a model built from the perspective of battery electrochemical reaction mechanism, which is mainly used in the development process of solid batteries and has a high degree of model complexity[12]. The neural network model is based on the theory of artificial neural network, and collects a large amount of effective experimental data by designing experiments on the battery, and then describes the internal and external characteristics of the battery.

The equivalent circuit model is based on the most basic circuit principles, and describes the response characteristics and internal characteristics of the battery through the combination of actual circuit components[13] (such as resistance, capacitance, inductance). Therefore, to build an accurate equivalent circuit model for a real battery, the following points should be achieved.

(1) Understand the reaction mechanism of the battery, accurately define the internal states of the battery such as SOC and polarization voltage, and accurately model the equation of state of the equivalent circuit model.

(2) To achieve the description of the battery response characteristics through the combination of circuit elements and to establish accurate measurement equations[14].

(3) Minimizing the number of circuit elements, thus increasing the actual engineering characteristics of the model.

The classical equivalent circuit models for battery SOC estimation are as follows: Rint model, PNGV model, Thevenin model, GNL model and so on.

In this paper, we choose a third-order battery model based on the Thevenin model.

The equivalent circuit model and its parameters, especially the parameters in the above section, are essential for the subsequent real-time simulation of the SOC algorithm. At the same time, however, a data-based battery model has been integrated in SIMULINK. The advantage of this model is that we do not need to simulate the parameters of the battery and can input the battery characteristics through the original parameter table of the battery. This allows the battery to simulate the real input and output of the battery pack very well when intervening in the vehicle model, without worrying about the impact of errors due to parameter identification.

2.1.2 Basic battery data

The battery we used for simulation is a 50Ah battery from Samsung, and by checking the relevant information, we were able to get some basic data of the battery.

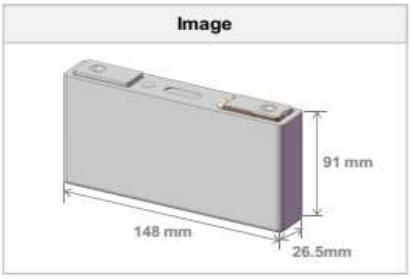

Mechanical Data

Dimensions	148L x 26.5W x 91H
Volume	0.357 L
Weight	875 g
Terminal type	Rivet
Terminal mat	Al / Al
Can material	Al
Can potential	Positive
OSD	Y
Fuse	Y
Vent	Y

Figure 2-1 Mechanical Data

Technical Data

Items		Data
Capacity	@25℃, ½C (min)	50 Ah
Voltage	@25℃, ½C (max/nominal/min)	4.25 V/ 3.68 V / 2.80 V
Energy	@25℃, ½C (min)	184 Wh
Specific energy	@25℃, ½C (min)	210 Wh/kg
Energy density	@25℃, ½C (min)	516 Wh/L
DC-IR	10s discharge@25℃, SOC 50%, BOL	1.40 mOhm
I_max	10s discharge@25℃	360 A
Power	10sec discharge@ 25℃,SOC50%, Vmin	1,624 W
	10sec discharge@ 25℃,SOC50%, Imax	1,145 W
	10sec charge@ 25℃,SOC50%, Imax	503 W
Cycle life	1C/1C@45℃, DOD 100%, EOL80%	1,200 cycles
Calendar life	@25℃, SOC100, EOL80%	10 yr
Operation temperature	Cycle	-30 ~ 60 ºC
	Storage	-40 ~ 60 ºC

Figure 2-2 Technical Data

By reading the above data, we conclude that the standard capacity of this battery is 50Ah, and the nominal voltage is 3.68V. Our solution is to use this battery to build a 2 parallel 28 series (2P28S) battery pack.

Also we know the internal resistance of the battery at -25 degrees, -10 degrees, 0 degrees, 10 degrees, 25 degrees and 40 degrees, according to the DC discharge for 30 seconds. As shown in the table 2-1 below.

Meanwhile, we know the internal resistance of the battery at -25 degrees, -10 degrees, 0 degrees, 10 degrees, 25 degrees and 40 degrees, according to the DC discharge for 30 seconds. As shown in the table 2-2 below.

At the same time, we have the relationship between OCV and SOC of this battery at 25 degrees Celsius. This will help us to get the SOC breakpoints and the corresponding terminal voltages of our battery model. This is very useful for us to obtain the relevant parameters of the equivalent circuit through simulation. Please see Figure 2-3 and Table 2-2 for the specific data.

SOC % Temp	90	80	70	60	50	40	30	20	10
40	1.57	1.55	1.54	1.49	1.40	1.52	1.53	1.77	2.47
25	1.91	1.88	1.86	1.85	1.77	1.78	1.94	2.73	3.68
10	2.60	2.50	2.54	2.55	2.46	2.51	2.73	3.91	6.59
0	3.40	3.35	3.36	3.41	3.31	3.42	3.73	5.67	12.46
-10	4.90	4.84	4.85	4.92	4.90	5.06	5.53	9.23	22.72
-25	9.43	9.29	9.30	9.45	9.34	9.70	11.06	20.28	53.49

Table 2-1 Internal resistance of DC discharge at different temperatures

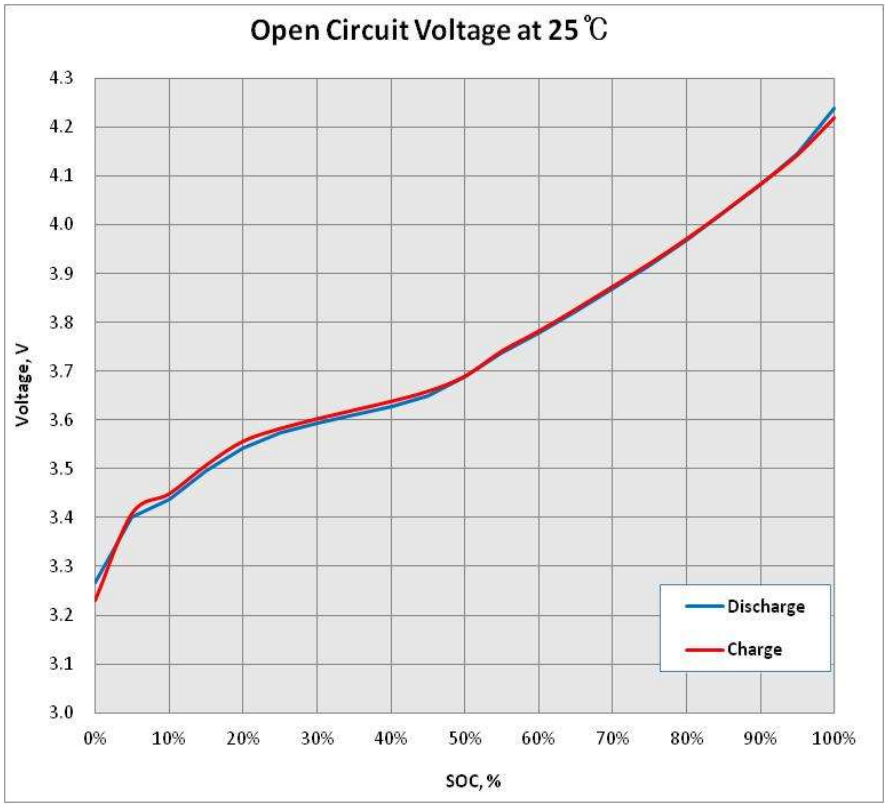

Figure 2-3 OCV versus SOC at 25°C

25°C	Discharge	Charge
100%	4.238	4.218
95%	4.146	4.142
90%	4.083	4.082
85%	4.024	4.025
80%	3.968	3.97
75%	3.917	3.92
70%	3.869	3.873
65%	3.823	3.826
60%	3.778	3.781
55%	3.736	3.740
50%	3.687	3.689
45%	3.649	3.658
40%	3.628	3.638
35%	3.611	3.620
30%	3.593	3.602
25%	3.574	3.582
20%	3.542	3.556
15%	3.496	3.507
10%	3.438	3.448
5%	3.401	3.409
0%	3.266	3.231

Table 2-2 OCV data under different SOC

2.2 SIMULINK Data-based battery pack model

With the use of the battery models that come with MATLAB-simulink, we can obtain a battery model that meets our different needs. These battery models can be built as a single cell or as a battery pack, depending on our experimental purpose and experimental needs. Here, based on the battery data we have at hand, we choose the DATA-BASED pack model, in which we can build a 2p28s battery pack by entering a series of parameters. The relevant parameters are selected as shown below.

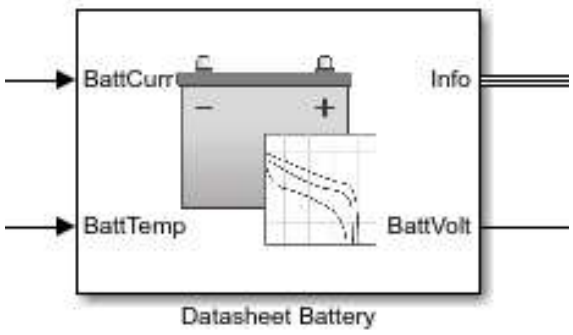

Figure 2-4 Datasheet Battery Block

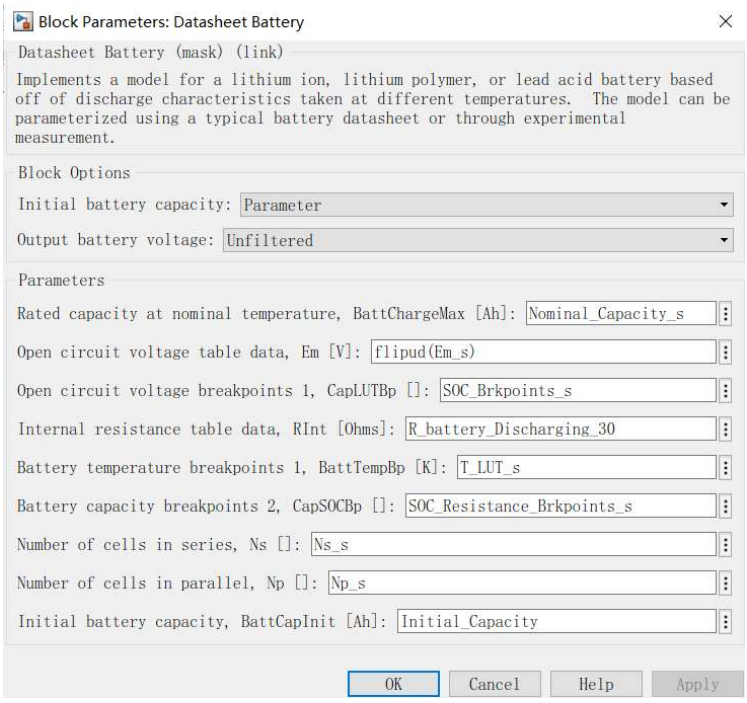

Figure 2-5 Data setting interface

Nominal Capacity	**50Ah**
Em	[4.238 4.146 4.083 4.024 3.968 3.917 3.869 3.823 3.778 3.736 3.687 3.649 3.628 3.611 3.593 3.574 3.542 3.496 3.438 3.401 3.266]
SOC breakpoints	(0:0.05:1)'
R-battery discharging	From Table 2-1
T-lookup table	[-25 -10 0 10 25 40]+273.15
SOC resistance breakpoints	[0.1 0.2 0.3 0.4 0.5 0.6 0.7 0.8 0.9]
Ns	28
Np	2
Initial Capacity	50Ah

Table 2-3 Parameter input table

After building this model, we input a pulse current with an amplitude of 100 to perform a simple test on the battery model, and we can obtain the following voltage image.

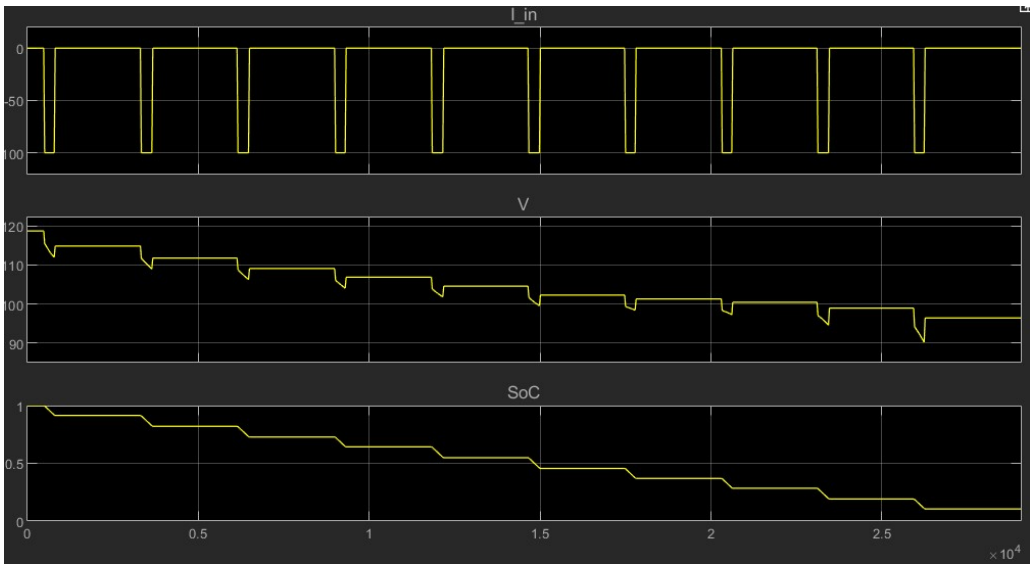

Figure 2-6 Input current, output voltage and its corresponding SOC

2.3 Third-order equivalent circuit model

2.3.1 Designing equivalent circuits

The equivalent circuit model of the battery is an external characteristic model, which is essentially an estimate of the dynamic characteristics of the battery using directly measured voltammetric parameters. The third-order RC network equivalent circuit model consists of a resistor and three first-order RC networks connected in series, as shown in Figure 2-7.

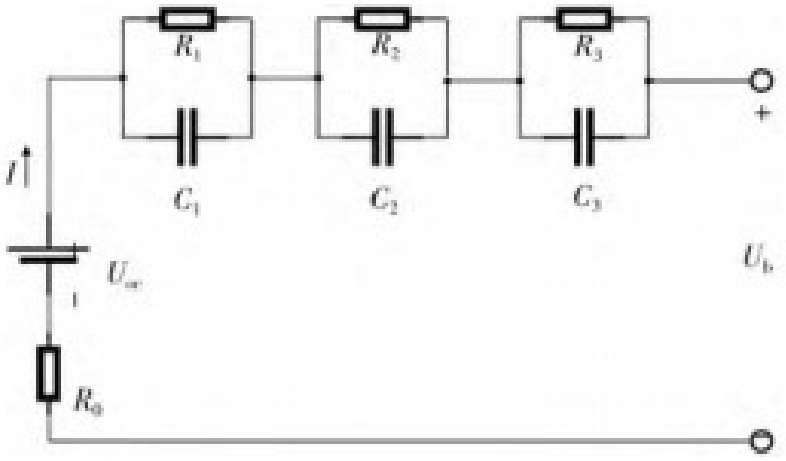

Figure 2-7 Third-order equivalent circuit diagram

In Figure 2-7, U_{oc} is the open-circuit voltage of the battery; U_b is the terminal voltage of the battery[15]; R_0 is the ohmic internal resistance of fixed resistance inside the battery; R_1 is the ohmic polarization resistance; R_2 is the electrochemical polarization resistance; R_3 is the concentration difference polarization resistance; C_1 is the ohmic polarization capacitance ; C_2 is the electrochemical polarization capacitance; C_3 is the concentration difference polarization capacitance. and U_1 , U_2

and U_3 are the voltages across capacitors C_1, C_2 and C_3, respectively; I is the current inside the model.

We can obtain the expressions for the voltage and current of each part of the equivalent impedance.

$$U_b = U_{oc} - IR_0 = U_1 - U_2 - U_3 \tag{2-1}$$

$$I = C_1 \frac{dU_1}{dt} + \frac{U_1}{R_1} \tag{2-2}$$

$$I = C_2 \frac{dU_2}{dt} + \frac{U_2}{R_2} \tag{2-3}$$

$$I = C_3 \frac{dU_3}{dt} + \frac{U_3}{R_3} \tag{2-4}$$

After we have learned the principle of the third-order RC circuit cell model, we can easily construct an equivalent circuit cell by using the Table-BASED cell model in SIMULINK.

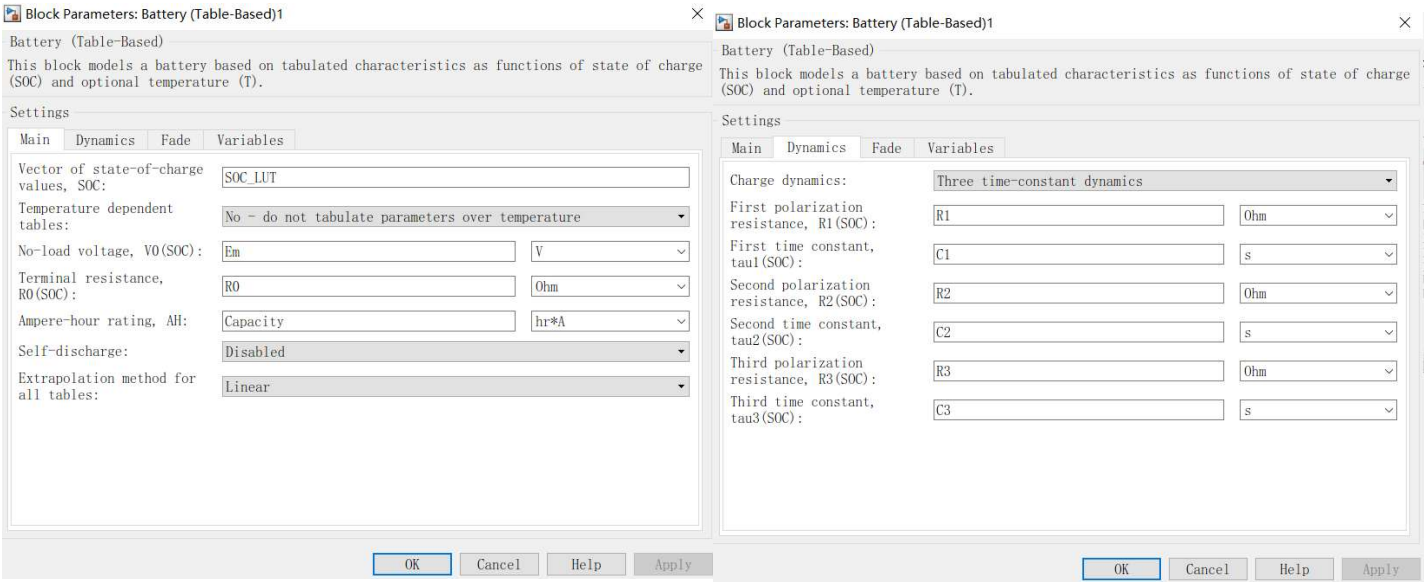

Figure 2-8 Parameter Setting

Since we do not know the exact value of R_0,R_1,R_2,R_3,C_1,C_2,C_3 here, we take an estimated value and set it as the initial condition. The specific numerical matrix will be calculated in the subsequent parameter estimation experiments.

2.3.2 Battery characteristic curve analysis

In order to better demonstrate the changes in voltage during the discharge-rest process and the basis for the identification of model parameters, the cycle section curves in Figure 2-6 were analyzed and the relevant measured data were recorded, and one of the curves (shown in the figure) was used to illustrate.

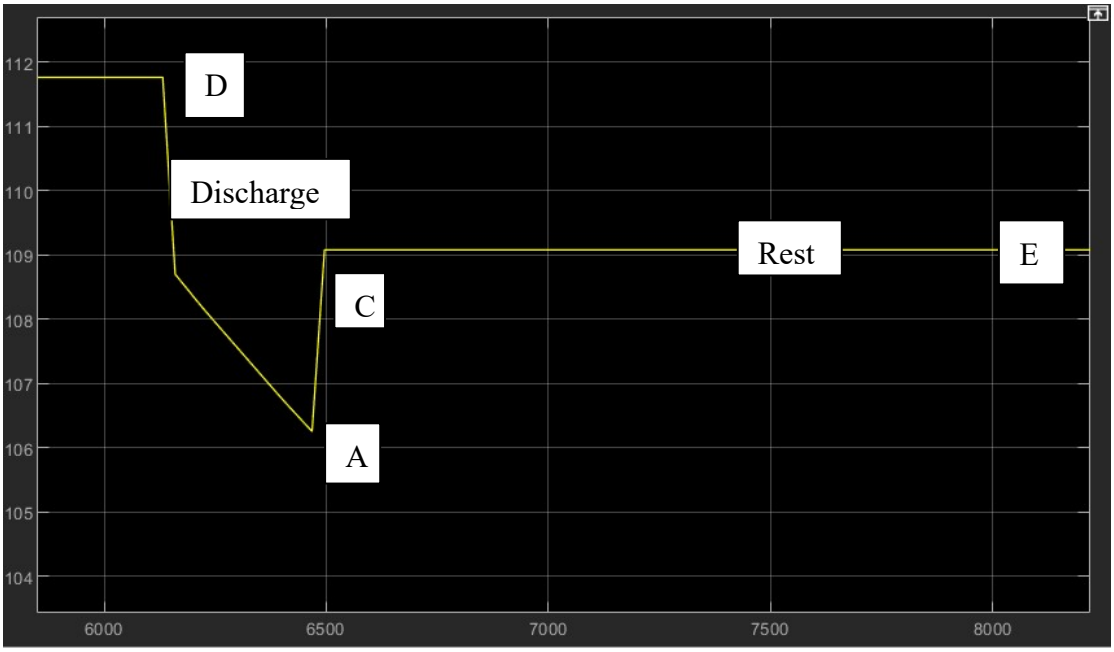

Figure 2-8 Static voltage recovery curve

Point D is the voltage at the beginning of discharge, section D - A is the discharge area, section A - E is the resting area, section A - C is the open-circuit voltage change of the battery due to ohmic internal resistance, section C - E is the open-circuit voltage change of the battery due to polarization impedance, because the resting time is long enough, the open-circuit voltage at point E is considered to be the equilibrium potential of the battery[17]. The open-circuit voltage at point E is considered to be the equilibrium potential of the battery due to the long standing time.

According to the rebound mechanism of voltage, when the battery stops discharging, the current flowing inside the battery suddenly becomes zero, and the

Li+ inside the battery will not be replenished in time to return to the equilibrium state through the diffusion stage and phase transition stage[18], which will show the open-circuit voltage of the battery rising sharply first, then rising slowly, and finally reaching the equilibrium state. From the experimental data and the reaction mechanism, it can be seen that both the impedance and capacitive resistance of the cell have an effect on the open-circuit voltage of the Li-ion battery.

2.4 Parameter Identification

2.4.1 Parameter estimation of ohmic internal resistance

As can be seen from Figure 2-8, each RC network in the model has a zero-state response in the D - A section[19]. Based on the circuit knowledge, the zero-state response function of the RC network is :

$$U(t) = I(t)R \times (1 - e^{-\frac{t}{CR}}) \tag{2-5}$$

In Eq.(2-5): $U(t)$ is the terminal voltage of the RC network; $I(t)$ is the real time current; t is the time, s.

Combining with the equivalent circuit model of a third-order RC network battery, starting from D (t_D = 0), the terminal voltage of the cell at any time in the region D - A is:

$$U(t) = Uoc - IR_0 - U_1(t) - U_2(t) - U_3(t)$$

$$= U_{oc} - IR_0 - IR_1(1 - e^{-\frac{t}{C_1R_1}}) - IR_2(1 - e^{-\frac{t}{C_2R_2}}) - IR_3(1 - e^{-\frac{t}{C_3R_3}}) \tag{2-6}$$

According to the "lithium-ion battery industry specifications

According to the "Lithium-ion Battery Industry Specification" and the internal resistance characteristics of large-capacity lithium-ion batteries , the resistances R1, R2 and R3 are generally in the range of a few milliohms to several tens of milliohms. and the values of capacitors C1, C2 and C3 are about10^3~10^5F. Therefore, the values of $\frac{t}{C_1R_1}$, $\frac{t}{C_2R_2}$ and $\frac{t}{C_3R_3}$ can be calculated to be about 0. Therefore according to

equation (2-6), the expression for the voltage at point A at the end of discharge can be written.

$$U_A = U_{OC} - IR_1 - IR_2 - IR_3 \tag{2-7}$$

The terminal voltages of the 3 RC networks at point A can be obtained.

$$U_1(A) = IR_1 \tag{2-8}$$

$$U_2(A) = IR_2 \tag{2-9}$$

$$U_3(A) = IR_3 \tag{2-10}$$

From Fig. 2-8, it can be seen that the current flowing outside the battery jumps to 0 when the battery discharge circuit is disconnected in section A-C. The state of the battery is changed and the open-circuit voltage suddenly rises, mainly due to the ohmic internal resistance of the fixed resistance inside the battery. Combined with the established third-order RC equivalent circuit model[19], this phenomenon is realized by the series resistance R_0 in the equivalent circuit model, that is, A → C (A, C time interval is very short, can be regarded as the same time) there is an ohmic voltage drop, R_0 can be calculated by equation (2-11)

$$R_0 = \left|U_c - U_a\right| / I \tag{2-11}$$

With the data in Fig. 2-6, the open-circuit voltages U_c , U_a and rebound voltages at points A and C at the instant after the battery is disconnected can be calculated. The ohmic internal resistance R_0 is calculated for different SOC values.

2.4.2 Parameter identification of polarization impedance

When the battery enters the resting stage from point C, the internal polarization characteristics of the battery, such as impedance and capacitive resistance characteristics, are affected, and chemical reactions are still carried out inside the battery until the final dynamic equilibrium is reached[20]. In the case of zero external current, the RC network analysis shows that the RC network is equivalent to zero

input response, if point C is the initial timing moment ($t_c = 0$), then the expression of RC network is:

$$U(t) = U(C)e^{-\frac{t}{CR}} \tag{2-12}$$

As can be seen from Figure 2-8, since the expression for the C-E section cannot be written intuitively, the values of the polarization impedances R_1, R_2 and R_3 and the polarization capacitances C_1, C_2 and C_3 need to be determined by means of a least squares fit. At the moment of disconnection (the time interval is very small and can be considered as the same moment), the voltage change of each RC network is very small and can be considered as U_1 (A) = U_1 (C) = IR_1, U_2 (A) = U_2 (C) = IR_2 and U_3 (A) = U_3 (C) = IR_3. The open-circuit voltage of the cell at any point in the C-E section is :

$$\begin{aligned} U(t) &= Uoc - U_1(t) - U_2(t) - U_3(t) \\ &= U_{oc} - U_1(C)e^{-\frac{t}{C_1R_1}} - U_2(C)e^{-\frac{t}{C_2R_2}} - U_3(C)e^{-\frac{t}{C_3R_3}} \\ &= U_{oc} - IR_1e^{-\frac{t}{C_1R_1}} - IR_2e^{-\frac{t}{C_2R_2}} - IR_3e^{-\frac{t}{C_3R_3}} \end{aligned} \tag{2-13}$$

Since the resting time is long, we can consider $e^{-\frac{t}{C_1R_1}}$, $e^{-\frac{t}{C_2R_2}}$ and $e^{-\frac{t}{C_3R_3}}$ as 0,so the voltage at point E is :

$$U(t_E) = U_{oc} - U_1(t_E) - U_2(t_E) - U_3(t_E) \tag{2-14}$$

The real-time voltage expression for the C - E section is :

$$U(t) = U(t_E) - IR_1e^{-\frac{t}{C_1R_1}} - IR_2e^{-\frac{t}{C_2R_2}} - IR_3e^{-\frac{t}{C_3R_3}} \tag{2-15}$$

The fit was performed with the following equation, and the fitting process was done in MATLAB.

$$U(t) = U(t_E) - a_1e^{-\tau_1 t} - a_2e^{-\tau_2 t} - a_3e^{-\tau_3 t} \tag{2-16}$$

Comparing equations 2-15 16, we get

$$\begin{aligned} R_1 &= a_1 / I \quad & C_1 &= I / (\tau_1 a_1) \\ R_2 &= a_2 / I \quad & C_2 &= I / (\tau_2 a_2) \\ R_3 &= a_3 / I \quad & C_3 &= I / (\tau_3 a_3) \end{aligned} \tag{2-17}$$

By using the least squares method, we can obtain the value of the above equation.

2.4.3 Results of parameter estimation

Bringing the above equation into MATLAB, the process of parameter estimation can be completed. Here is the specific settings screen .

```
% Em open-circuit voltage vs SOC
Em = 118*ones(size(SOC_LUT)); %Volts
% R0 resistance vs SOC
R0 = 0.01*ones(size(SOC_LUT)); %Ohms
% R Resistance vs SOC
R1 = 0.0005*ones(size(SOC_LUT)); %Ohms
R2=0.0005*ones(size(SOC_LUT));
R3=0.0005*ones(size(SOC_LUT));
% C Capacitance vs SOC
C1 = 10*ones(size(SOC_LUT)); %Farads
C2=100*ones(size(SOC_LUT));
C3=500*ones(size(SOC_LUT));
```

Figure 2-9 Initial starting points before estimation

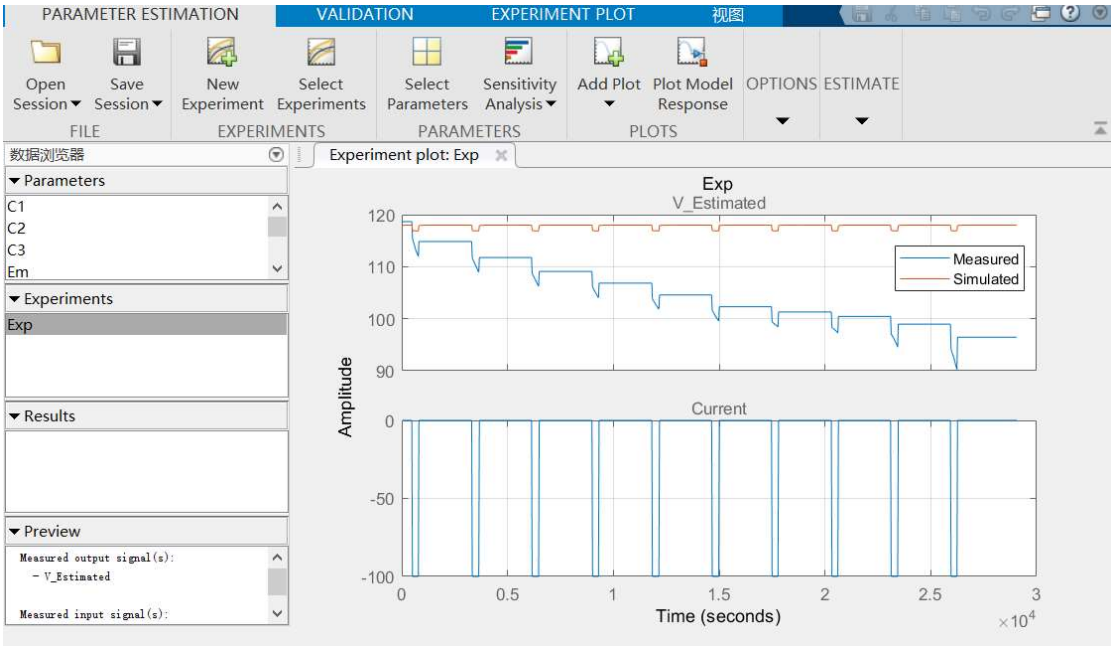

Figure 2-10 Parameter estimation initial state

This is the parameter estimation initial state image. We can see the huge difference between the voltage output due to our random initial parameters and the real voltage output when we did not perform parameter fitting. This difference will gradually decrease as we proceed with the parameter fitting. Until the two curves coincide almost perfectly, we will have the specific parameters of the third-order equivalent circuit of the pack.

The parameter fitting curve after iteration is shown here

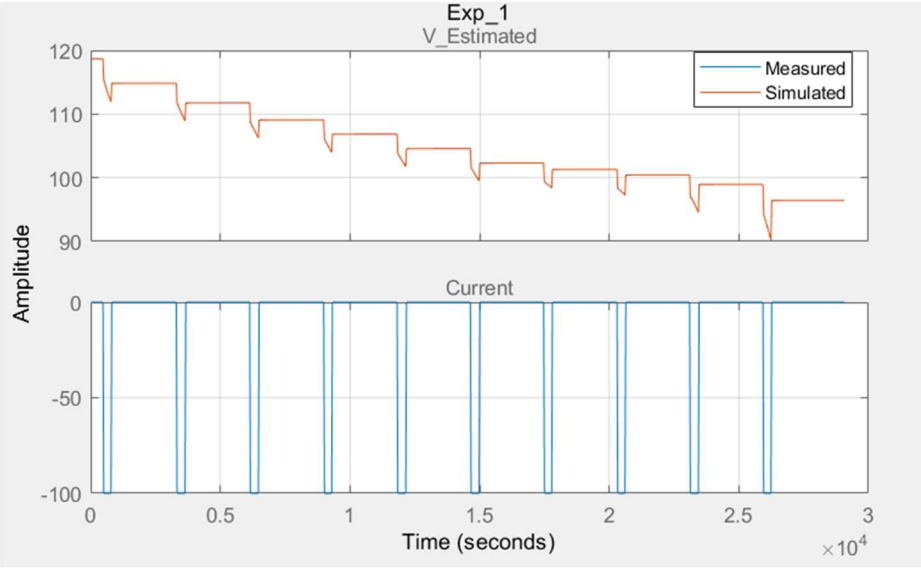

Figure 2-11 Fitting curve after estimation

After iteration, we can obtain the specific parameters as shown in the following table.

SOC(%)	Em	R_0	R_1	R_2	R_3	C_1	C_2	C_3
100	118	0.01	0.0005	0.0005	0.00051809	10	100	500
95	118	0.01	0.0005	0.0005	0.00056203	10	100	500
90	96.626	0.066927	0.00070223	0.00058717	0.00052487	9.9656	98.284	491.65
85	95.054	0.025482	0.00057616	0.000651	0.00052962	9.9524	97.581	485.75
80	99.796	0.04858	0.00063282	0.00056574	0.00051077	9.8746	98.121	490.82
75	98.617	0.021924	0.0005496	0.00057674	0.00052022	9.9653	98.043	492.58
70	101.27	0.036364	0.00059439	0.00054688	0.00050097	9.9379	98.226	495.09
65	101.33	0.031041	0.00058101	0.00056949	0.00050621	9.9436	96.861	493.41
60	101.27	0.024036	0.00055142	0.00052598	0.00049748	9.968	98.735	498.3
55	102.36	0.029391	0.00056989	0.00053791	0.00050112	9.8894	97.444	496.49
50	101.84	0.01286	0.0005098	0.00050615	0.0005036	9.9839	99.717	500.19
45	104.65	0.028296	0.00056267	0.00052115	0.00050366	9.891	98.52	497.83
40	104.36	0.01388	0.00051427	0.0005169	0.00051415	9.9795	99.545	498.89
35	107.32	0.030967	0.0005731	0.00052778	0.00050424	9.9189	98.654	497.16
30	108.1	0.025981	0.00056028	0.00055005	0.00051565	9.9567	97.948	495.21
25	109.87	0.02997	0.00057311	0.00053624	0.00050086	9.954	98.563	496.95
20	111.34	0.030838	0.00057836	0.000559	0.00051084	9.9397	97.156	494.3
15	112.36	0.025229	0.00055556	0.00052734	0.00049618	9.9635	98.763	498.09
10	114.71	0.03295	0.00058529	0.0005518	0.00050499	9.9098	96.897	495.2
5	115.16	0.019326	0.00053122	0.0005113	0.00051809	9.9611	99.104	499.76

0	118.68	0.030678	0.00057282	0.0005304	0.00056203	9.8312	98.01	498.66

Table 2-4 Parameter Value

2.5 Battery pack operating platform

As previously described, the application scenario for our battery is the EV model of the classic Panda, which has an electrical SIMULINK simulation platform built by Professor Mr. Stefano. The specific SIMULINK image is shown in the figure 2-.

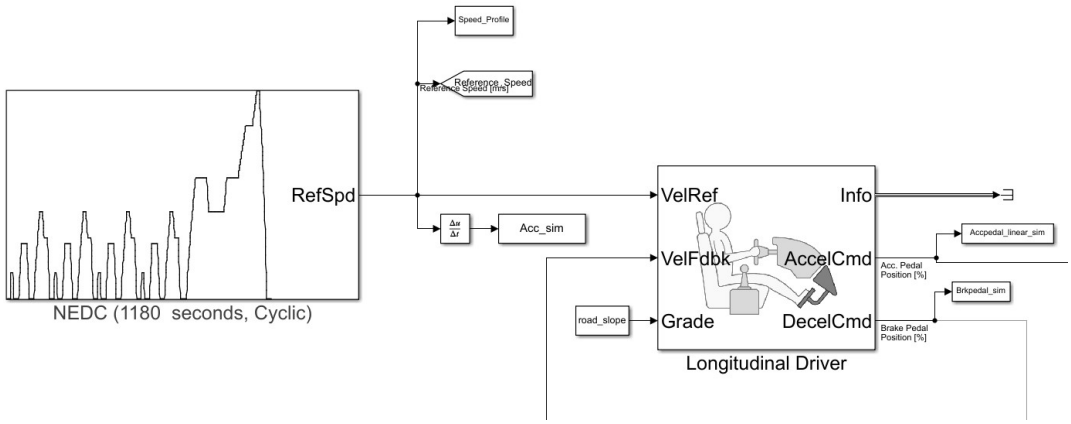

Figure 2-12 Simulated driver section

This is the part where we pre-enter the loop we want. and "force" the simulated driver system to produce a pedal behavior appropriate to this cycle. In a purely electric vehicle, the change in pedal behavior can be seen as a change in current.

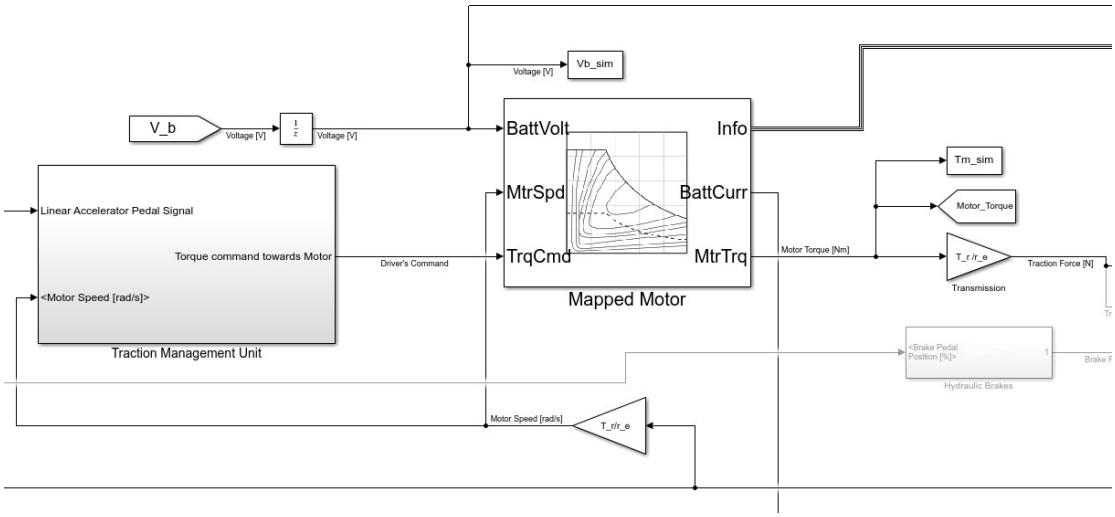

Figure 2-13 Traction Management Unit

The role played by this part is to simulate the generation of traction by the car. After following the path followed in the previous module, we can get the traction force we need to generate and the current flowing through the vehicle circuit and output the signal here.

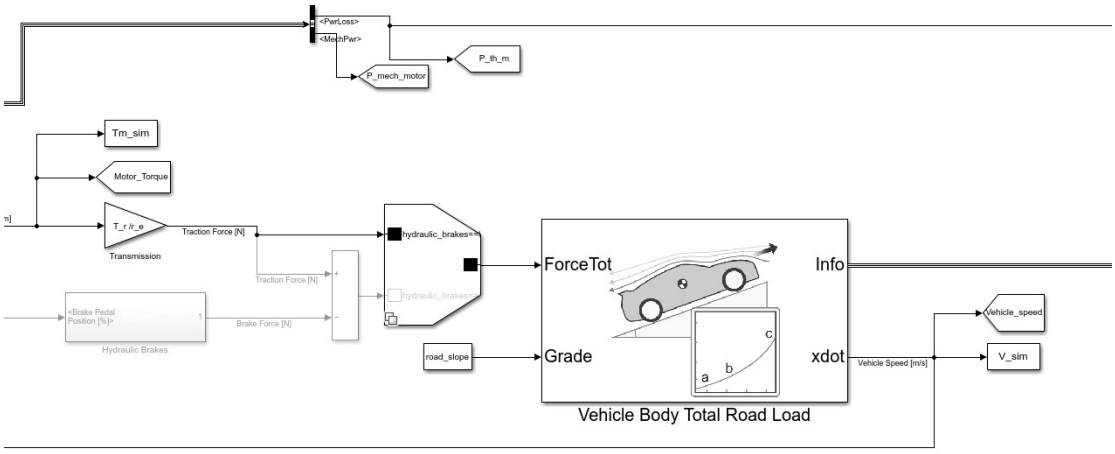

Figure 2-14 Road load section

This part serves to simulate the feedback given to the vehicle by the road surface. It also simulates the intervention of the vehicle's brake pedal. The hydraulic braking module here can also carry a kinetic energy recovery role, which means that our

vehicle can generate a current to charge the battery pack when braking in the opposite direction to the forward direction. This will be reflected in the subsequent energy consumption analysis.

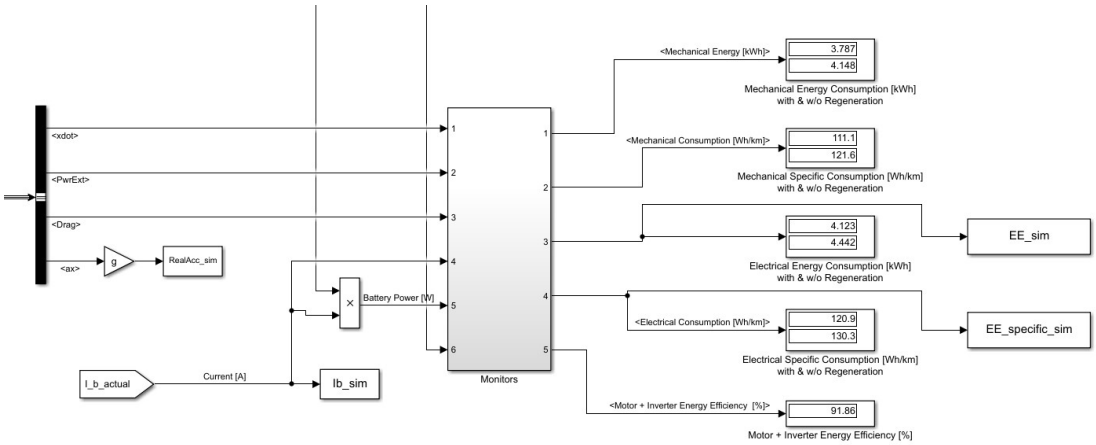

Figure 2-15 Data monitoring module

The purpose of this module is to collect data from the previous boards for us to analyze. Data is maintained for subsequent work.

The complete vehicle modeling block diagram will be given in the appendix.

2.6 Summary of this chapter

In this chapter, we focus on the current mainstream battery simulation models. For our simulation object, we construct a third-order RC equivalent circuit model for the Thevenin battery model, which is too simple in structure and not high in accuracy. The model has a moderate complexity and high accuracy, which can reflect the dynamic polarization impedance of the battery well and simulate the real-time operating characteristics of the battery.

The relationship between the equilibrium electric potential and SOC is obtained through the battery charging and discharging performance test, and the rebound voltage experiment is designed to obtain the relationship between the battery impedance and SOC, and the internal polarization impedance of the battery is accurately estimated by the least squares method in SIMULNK based on the experimental data.

CHAPTER 3

Estimation of SOC based on Kalman filtering

3.1 Classical Kalman filtering

In 1960, R.E. Kalman proposed a recursive approach to solving the problem of linear filtering of discrete data in his Ph.D. thesis. Subsequently, this method was developed and extended to cases such as nonlinear filtering and is widely used in applications such as navigation and localization[21]. In recent years, the Kalman filter algorithm has been applied to battery SOC estimation, resulting in a significant improvement in estimation accuracy.

The Kalman filter method is a time-domain method. It introduces the concept of state variables, describes the dynamic system with state equations, describes the observed information with measurement equations, and replaces the transfer function model used in the previous Wiener filtering method with a state-space model. Among them, the accuracy of the state equation and the measurement equation will directly affect the filtering results.

The schematic diagram of the Kalman filter is shown in Figure 3-1. Considering a linear discrete-time constant stochastic system.

$$x(k+1) = \Phi x(k) + \Gamma w(k) \tag{3-1}$$

$$y(k) = Hx(k) + v(k) \tag{3-2}$$

where $x(k) \in R^n$, denotes the state vector of the system at time k. $y(k) \in R^m$, is the observation at time k. Γ, Φ, H is the constant array, $w(k) \in R^r$ and $v(k) \in R^m$, characterize the process noise and measurement noise of the system, respectively.

Suppose $w(k)$ and $v(k)$ are independent white noise with zero mean and variance array of Q and R each, and the initial state state $x(0)$ independent of $w(k)$ and $v(k)$, then the Kalman filter algorithm is computed as follows.

Initialization calculation

$$k = 0, x(0 \mid 0) = E(x(0)) = \mu_0 \tag{3-3}$$

$$P(0 \mid 0) = E\left[(x(0) - \mu_0)(x(0) - \mu_0)^T \right] = P_0 \tag{3-4}$$

$$Q = E(w(k) \times w(k)^T), R = E(v(k) \times v(k)^T) \tag{3-5}$$

Recursive calculation

$$\hat{x}(k+1 \mid k) = \Phi \hat{x}(k \mid k) \tag{3-6}$$

$$\varepsilon(k+1) = y(k+1) - H\hat{x}(k+1 \mid k) \tag{3-7}$$

$$P(k+1 \mid k) = \Phi P(k \mid k)\Phi^T + \Gamma Q \Gamma^T \tag{3-8}$$

$$K(k+1) = P(k+1 \mid k)H^T \left[HP(k+1 \mid k)H^T + R \right]^{-1} \tag{3-9}$$

$$P(k+1 \mid k+1) = \left[I_n - K(k+1)H \right] P(k+1 \mid k) \tag{3-10}$$

$$\hat{x}(k+1 \mid k+1) = \hat{x}(k+1 \mid k) + K(k+1)\varepsilon(k+1) \tag{3-11}$$

where I_n is the nth order unit matrix and E is the mathematical expectation.

3.2 Extended Kalman filtering

The Extended Kalman Filter (EKF) is a more widely used nonlinear filtering algorithm. As mentioned in the previous section, the classical Kalman filter algorithm can only be applied to linear systems. In order to apply the ideas of the Kalman filter algorithm to nonlinear systems, the EKF algorithm uses the Taylor expansion and omits the higher order terms to approximate the nonlinear model to a linear model,

and then follows the process of the classical Kalman filter algorithm to complete the filtering form.

The EKF algorithm can be widely applied to a variety of nonlinear systems, and can achieve good state estimation for systems with weak nonlinearity. The EKF algorithm can be applied to a wide range of nonlinear systems, and can achieve good state estimation for systems that are not strongly nonlinear[22].

For a typical nonlinear system, the model equation can be written as:

$$x_k = f(x_k, u_k) \tag{3-12}$$

$$y_k = g(y_k, u_k) \tag{3-13}$$

x_k is the system state variable, y_k is the system observed variable, u_k is the input variable to the system, $f(x_k, u_k)$ is a nonlinear function related to the state of the system; $g(y_k, u_k)$ is a nonlinear function related to the state variable x_k and the observed quantity y_k .

At each point in time, $f(x_k, u_k)$ and $g(y_k, u_k)$ are linearized using a first-order Taylor expansion. at each point in time. Setting $f(x_k, u_k)$ and $g(y_k, u_k)$ to be differentiable at each selected sampling point, we have；

$$f(x_k, u_k) \approx f(\tilde{x}_k, u_k) = \frac{\partial f(x_k, u_k)}{\partial x_k}|_{x_k = \bar{x}_k} (x_k - \tilde{x}_k) \tag{3-14}$$

$$g(x_k, u_k) \approx g(\tilde{x}_k, u_k) = \frac{\partial g(x_k, u_k)}{\partial x_k}|_{x_k = x_k} (x_k - \tilde{x}_k) \tag{3-15}$$

Set $\tilde{A}_k = \frac{\partial f(x_k, u_k)}{\partial x_k}|_{x_k = \bar{x}_k}$, $\tilde{C}_k = \frac{\partial g(x_k, u_k)}{\partial x_k}|_{x_k = \bar{x}_k}$

Then the expression for the linearization of a nonlinear system related only to the state vector is derived as:

$$x_{k+1} \approx \tilde{A}_k x_k + \left[f(\tilde{x}_k, u_k - \tilde{A}_k x_k) \right] + w_k \tag{3-16}$$

$$y_k \approx \tilde{C}_k x_k + \left[g(\tilde{x}_k, u_k - \tilde{C}_k x_k) \right] + v_k \tag{3-17}$$

w_k , v_k are the state equation noise and measurement equation noise[23], respectively, and are mutually independent Gaussian white noise with zero mean of Gaussian white noise,so $w_k \sim N(0, Q_k)$ and $v_k \sim N(0, R_k)$, Q_k is the state equation noise covariance, and $Q_k = E(w_k, w_k^T)$, and R_k is the measurement equation noise covariance, $R_k = E(v_k, v_k^T)$.

The specific steps of the extended Kalman filter are shown below.

a) Initialization: at the moment *k - 1*, the

$$\tilde{x}_{k-1} = E\left[x_{k-1}\right], P_{k-1} = E\left[(x_{k-1} - \tilde{x}_{k-1})(x_{k-1} - \tilde{x}_{k-1})^T \right] \tag{3-18}$$

b) Prediction

State prediction equation:

$$\tilde{x}_k^- = f(\tilde{x}_{k-1}, u_k) \tag{3-19}$$

State covariance prediction equation:

$$P_k^- = \tilde{A}_{k-1} P_{k-1} \tilde{A}_{k-1}^T + Q_{k-1} \tag{3-20}$$

c) Calibration

Feedback gain equation:

$$K_k = P_k^- \tilde{C}_k^T (\tilde{C}_k P_k^- \tilde{C}_k^T + R_k)^{-1} \tag{3-21}$$

The filtering equation:

$$\tilde{x}_k = \tilde{x}_k^- + k_k(y_k - g(\tilde{x}_k^-, u_k)) \tag{3-22}$$

Error covariance matrix update equation

$$P_k = (I - K_k H_k)P_k^- \tag{3-23}$$

The EKF algorithm is very similar to the KF filter algorithm as shown in equations (3.18) to (3.23) above. The difference is that the nonlinear state equation is used to calculate the time update of the state variables[24]. The nonlinear observation equation is used to calculate the vector estimate of the output $\tilde{y}_k = g(\tilde{x}_k^-, u_k)$, and the model linearization approximation determines A_k and C_k .

However, for strongly nonlinear systems, the performance of the EKF algorithm is extremely unstable and even generates divergence.

(2) The EKF algorithm requires the calculation of Jacobian matrix, which is complicated and prone to

(2) The computation of Jacobian matrix in the EKF algorithm is complicated and error-prone .

3.3 Unscented Kalman Filter

Due to the shortcomings of the extended Kalman filtering technique in processing nonlinear systems, the EKF is not negligible in the filtering process. The impact of errors in the filtering process cannot be neglected, so there is a need to find better ways to solve the problems encountered in the state estimation of nonlinear systems. The problems encountered in the state estimation of nonlinear systems. The Unscented Kalman filter is a nonlinear system estimation method that has gradually emerged in recent years. Unlike the linearized approximation of nonlinear systems by the traditional EKF method[25], the UKF algorithm uses a probability distribution approach to deal with nonlinear problems. It is the most promising nonlinear estimation method.

3.3.1 UT Transformation

The Unscented Kalman filter algorithm UKF is a derivative of the Kalman filter KF algorithm, which is known as the UKF algorithm when the UT transform is used to handle the nonlinear transfer of mean and covariance for a one-step prediction equation. The Unscented Transform is the core of the UKF algorithm, a method of varying a nonlinear function by computing the statistical values of nonlinear random variables.

The basic principle of the UT variation is to approximate the probability density distribution of the nonlinear function on the premise of obtaining the optimal value at the previous moment. In this case, a set of Sigma points is selected, ensuring that this point set has the same sampling mean and covariance, and the nonlinear variation is performed for each Sigma point in the point set, and the final point set and variance after the nonlinear variation are obtained. As shown in Figure 3-1, the difference between UKF and EKF for nonlinear problems is illustrated in the figure.

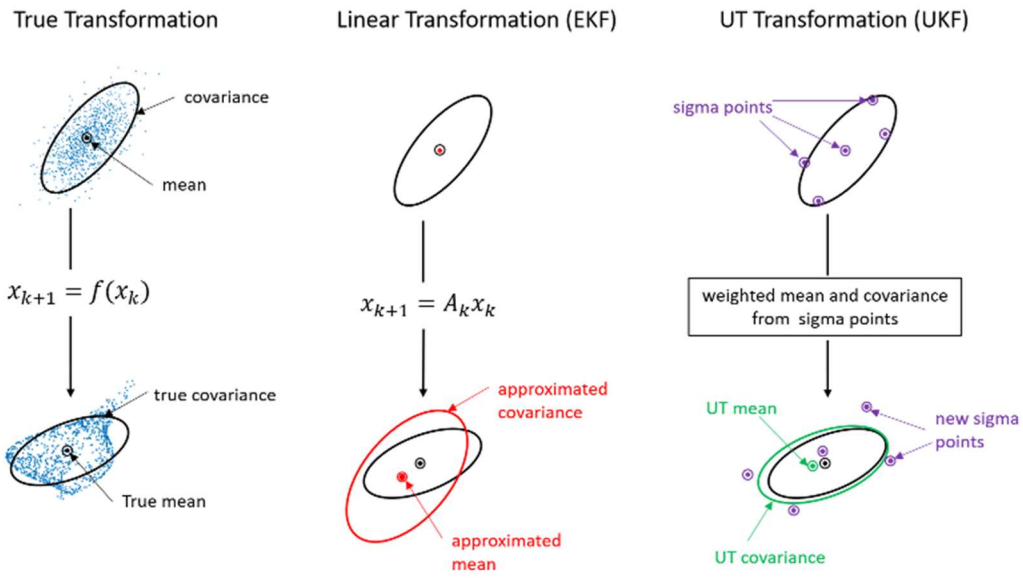

Figure 3-1 The difference between UKF and EKF

Determining the sampling strategy of Sigma points is the core of the UT transformation process, and the strategy is to determine the number of Sigma points, their positions, and the calculation of the corresponding weights. At present, the more mature Sigma point sampling strategies include monomorphic sampling, symmetric sampling, 3rd order moment skewness sampling, and Gaussian distribution 4th order moment symmetric sampling, etc., but the most commonly used in practical applications is still symmetric sampling.

The computational flow of the UT transform is as follows:

(1) For the input random variable *x*, the Sigma point sampling strategy is selected and its statistics are used to construct the Sigma point set $\{x_i\}, i=1...L$, and the corresponding weights W_i^m and W_i^c. where L is the number of sampled Sigma points, W_i^m is the weight used for mean weighting, and W_i^c is the weight used for covariance weighting. which are determined by the sampling strategy.

(2) The Sigma points in the Sigma point set $\{x_i\}$ constructed in (1) are transformed nonlinearly to obtain the transformed point set. $\{y_i\}, y_i = f(x_i)$

(3) For the point set $\{y_i\}$, the statistical information of the output variables (mean $\overline{y}$ and variance P_{yy}) are obtained with the weights W_i^m and W_i^c, respectively.

$$\overline{y} = \sum_{i=1}^{L} W_i^m y_i \tag{3-24}$$

$$P_{yy} = \sum_{i=1}^{L} W_i^c (y_i - \overline{y})(y_i - \overline{y})^T \tag{3-25}$$

3.3.2 Unscented Kalman filtering algorithm

Based on the UT transformation, the detailed steps of the UKF algorithm are.

a) Given the initial state.

$$\hat{x}_0 = E[x_0], P_0 = E\left[(x_0 - \hat{x}_0)(x_0 - \hat{x}_0)^T\right] \tag{3-26}$$

b) State dilation: As the interfering term needs to be estimated during the process, it should be doped.

$$\tilde{x}_0^a = E\left[x_0^a\right] = E\left[x_0 \quad v_0 \quad n_0\right] = \left[\tilde{x}_0 \quad 0 \quad 0\right] \tag{3-27}$$

$$P_0^a = E[(x_0^a - \overline{x}_0^a)(x_0^a - \overline{x}_0^a)^T] = \begin{bmatrix} P_0 & 0 & 0 \\ 0 & P_v & 0 \\ 0 & 0 & P_n \end{bmatrix} \tag{3-28}$$

c) Calculation of sampling points.

$$\chi_{0,k-1} = \tilde{x}_{k-1}^a \tag{3-29}$$

$$\chi_{i,k-1} = \tilde{x}_{k-1}^a + (\sqrt{(N+\lambda)P_{k-1}})_i, i = 1,\ldots,L \tag{3-30}$$

$$\chi_{i,k-1} = \tilde{x}_{k-1}^a - (\sqrt{(N+\lambda)P_{k-1}})_i, i = L+1,\ldots,2L \tag{3-31}$$

$$W_0^{(m)} = \lambda / (L+\lambda) \tag{3-32}$$

$$W_0^{(c)} = \lambda / (L+\lambda) + (1-\alpha^2+\beta) \tag{3-33}$$

$$W_i^{(m)} = W_i^{(c)} = 1/\left[2(L+\lambda)\right], i = 1,\ldots,2L. \tag{3-34}$$

$$\chi_{k-1}^a = \left[\tilde{x}_{k-1}^a, \tilde{x}_{k-1}^a + (\sqrt{(N+\lambda)P_{k-1}}), \tilde{x}_{k-1}^a - (\sqrt{(N+\lambda)P_{k-1}})\right] \tag{3-35}$$

$$\lambda = \alpha^2(L+k) - L \tag{3-36}$$

α is used to set the distance of these point sets to the mean, which is usually set to a small positive number. The distance to the mean can be controlled by the scalar *k*, which is usually set to 0 or 3-*n*, where *n* is the system is the order of the system. β is used to incorporate the prior information of the random variable *x*. For a Gaussian distribution, $\beta = 2$ is optimal[25]. Therefore, the parameters in the above equation are defined as: α*=1e-3,* β*=0, k=0*, and they are applicable in most cases.

d) Time update: propagates Sigma points backwards

$$\chi_{k|k-1}^{x} = F(\chi_{k-1}^{i}), i = 0, \cdots, 2L \tag{3-37}$$

The predicted values of the states and their variances are then calculated by combining the weights of the Sigma points

$$\tilde{x}_{i}^{-} = \sum_{i=0}^{2L} W_{i}^{(m)} \chi_{i,k|-1}^{x} \tag{3-38}$$

$$P_{x}^{-} = \sum_{i=0}^{2L} W_{i}^{(c)} (\chi_{i,k|k-1}^{x} - \tilde{x}_{k}^{-})(\chi_{i,k|-1}^{x} - \tilde{x}_{k}^{-})^{T} \tag{3-39}$$

e) Measurement update

Calculate the predicted value of the output and its variance

$$y_{k|k-1}^{x} = H(\chi_{klk-1}^{x}, \chi_{k|k-1}^{n}) \tag{3-40}$$

$$\tilde{y}_{k}^{-} = \sum_{i=0}^{2L} W_{i}^{(m)} y_{i,kk-1} \tag{3-41}$$

$$P_{\tilde{y}_k, \tilde{y}_k} = \sum_{i=0}^{2L} W_{i}^{(c)} (y_{i,k|k-1} - \tilde{y}_{i})(y_{i,k|k-1} - \tilde{y}_{i}^{-})^{T} \tag{3-42}$$

$$P_{\tilde{\chi}_k, \tilde{y}_k} = \sum_{i=0}^{2L} W_{i}^{(c)} (\chi_{i,k|k-1} - \tilde{y}_{i})(y_{i,k|k-1} - \tilde{y}_{i}^{-})^{T} \tag{3-43}$$

Calculate a posteriori estimates using actual output corrections:

$$\tilde{y}_{k} = z_{k} - \tilde{z}_{k|k-1} \tag{3-44}$$

$$\kappa = P_{x_k y_k} P_{\tilde{y}_k \bar{x}_k}^{-1} \tag{3-45}$$

$$\tilde{x}_k = \tilde{x}_k^- + \kappa(y_k - \tilde{y}_k^-) \tag{3-46}$$

$$P_k = P_k^- - \kappa P_{\bar{y}_k \bar{y}_k} \kappa^T \tag{3-47}$$

Through analysis, the UKF algorithm has the following advantages: for the state estimation of nonlinear systems, the mean accuracy of UKF estimation is higher than that of EKF, which can provide more accurate estimates of the state mean and state covariance[26,27]. Since the distribution of states in the UKF is not an approximation to a nonlinear function, the expansion of state levels is not a truncation to a specific order, so the UKF can better preserve higher order information and obtain higher computational accuracy than the EKF.

At the same time, because the EKF requires a derivable model, the UKF only uses vector and matrix operations to calculate the mean and variance, so it is suitable for arbitrary process models and does not need to calculate Jacobian matrices, which shows that the UKF has a broader scope of application and is relatively suitable for computation, and is easier to implement in hardware than the EKF.

3.4 Summary of this chapter

The main content of this chapter is to introduce the basic principles of Kalman filtering. The main contents of classical Kalman filtering, extended Kalman filtering and tasteless Kalman filtering and their computational procedures are introduced respectively. The principle and the role of UT transform are highlighted. A solid theoretical foundation is laid for establishing the relevant models in the later chapters.

CHAPTER 4

Real-time SOC and SOH estimation analysis based on UKF and EKF

4.1 SOC estimation through EKF Algorithm

Having studied the theoretical foundations in the previous chapter, we can now proceed to build our measurement system. First we will use the EKF to estimate the real-time SOC and R_0.

4.1.1 Estimation of SOC logic diagram by EKF

By understanding and implementing the equations in the previous chapter, we can know that to estimate the SOC of the battery pack and even the vehicle by the EKF method, we need to establish the following logical framework.

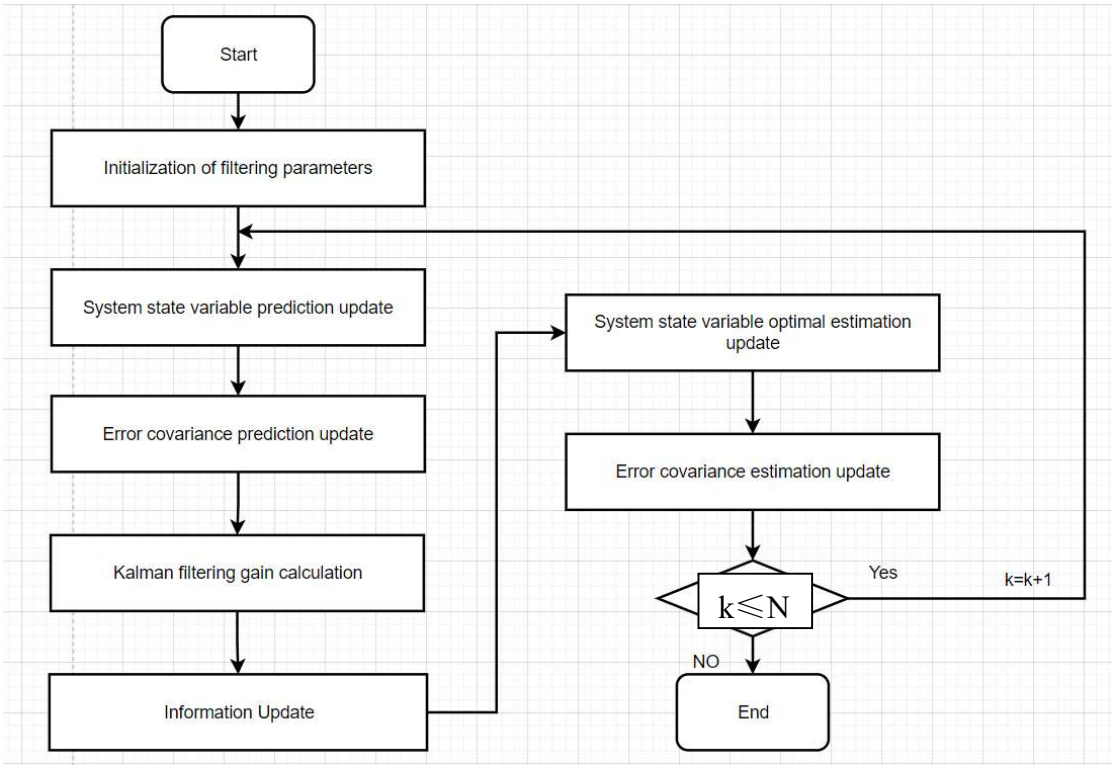

Figure 4-1 EKF algorithm logic diagram

The above computational process shows that the EKF algorithm is essentially a recursive process of predicting and correcting the system state variables so that the system estimates gradually converge to near the exact values.

During normal operation of the battery system, the load current flowing through the battery and the terminal voltage of the battery are finite and measurable. Therefore, the current is used as the input variable of the model in the EKF algorithm to drive the variation of the internal parameters of the model; the polarization voltage of the two parts of the resistive-capacitance network inside the battery equivalent circuit model and the battery state of charge SOC are used as the state variables of the system.

The terminal voltage of the battery is taken as the output variable of the system, and the output is obtained according to the structure of the battery equivalent circuit model and the E-SOC relationship obtained from the identification.

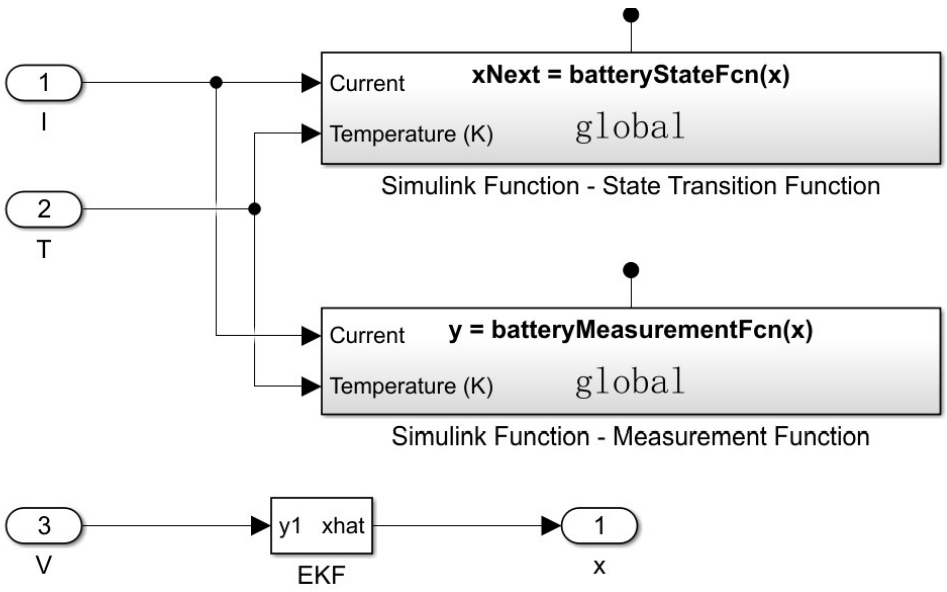

Figure 4-2 EKF modules

In addition, the initial values of some parameters need to be set when starting the EKF algorithm for battery charge state SOC estimation. Although the EKF algorithm is robust with low initial parameter accuracy, too much deviation will affect the convergence speed of the algorithm when estimating the state variables, which may cause the estimation results to be scattered in extreme cases[28].

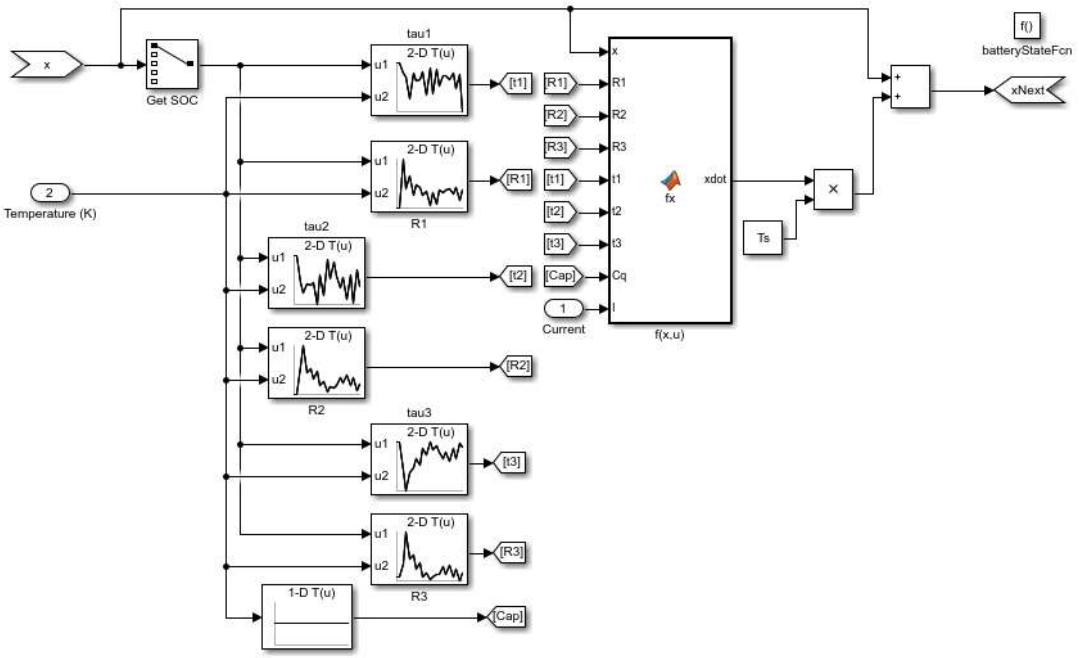

Figure 4-3 EKF State Transition Function

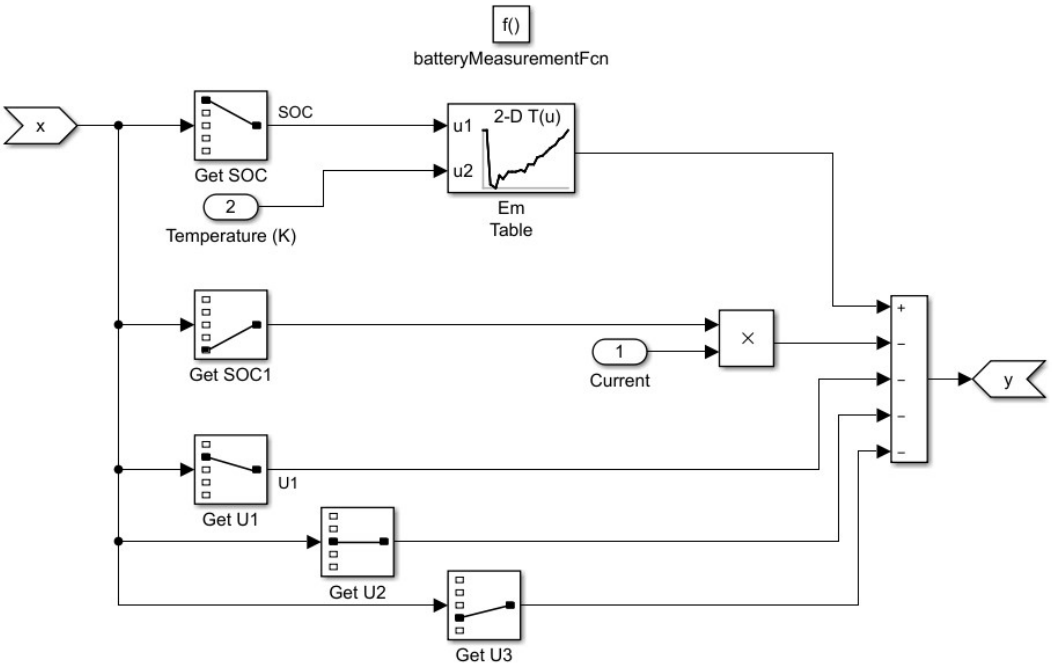

Figure 4-4 EKF Measurement Function

Since the battery is in a static state before operation, the initial values of U is equal to 0. The initial values of the charge state can be obtained according to the table

search data in Chapter 3, and the battery is not fully charged before the experiment, i.e., SOC(0)=0.9; the error covariance matrix P_0 is generally P_0 is generally set to a smaller value that is not zero, which indicates the deviation of the predicted value of the state variable from the true value, when the value of P0 is larger, it means that the current predicted value deviates more from the true value, and then the filter gain coefficient is also larger, so that the state variable can be corrected to a larger extent.

In the experimental process, the measurement noise v_k of the system is related to the accuracy of the sensor of the collected data, which is generally interspersed with the measurement data; similarly, the process noise ω_k is mainly caused by the accuracy of the established model, which is unavoidable. In setting the covariance R_k of the measurement noise and the covariance Q_k of the process noise, the tuned empirical values are usually taken.

4.1.2 Monitoring results

First, we chose WTP3 as our following simulation test mode. The speed requirements of this mode for our vehicle are shown in the figure below.

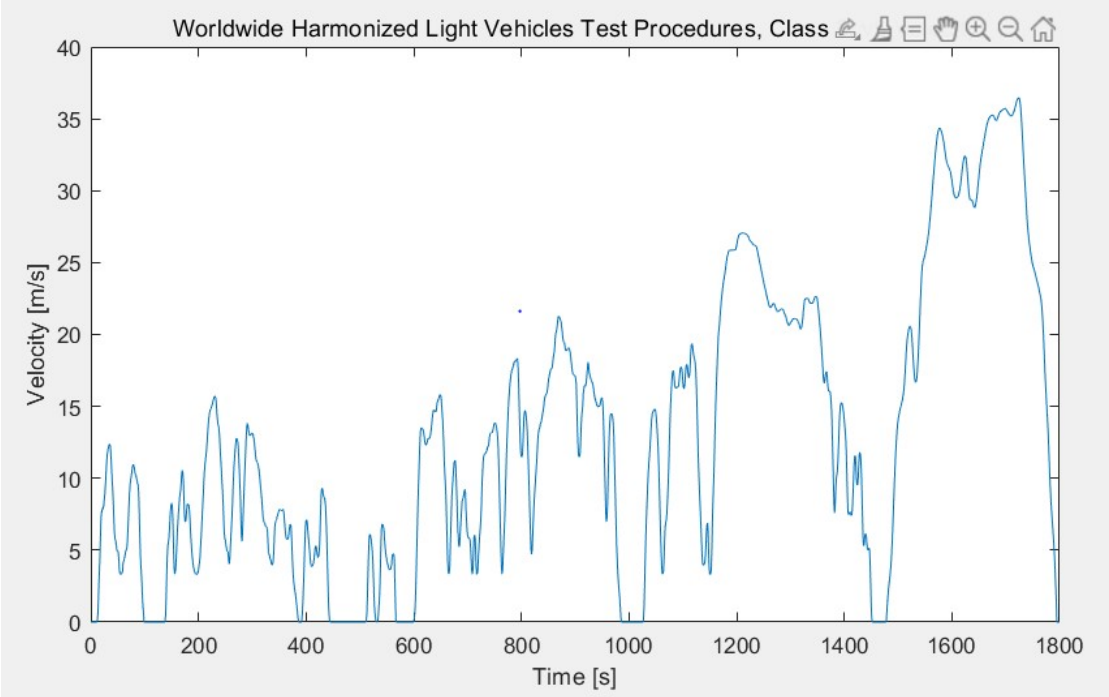

Figure 4-5 WTP3 Speed Diagram

For this speed route, the current image we need is shown below. We take two test loops here.

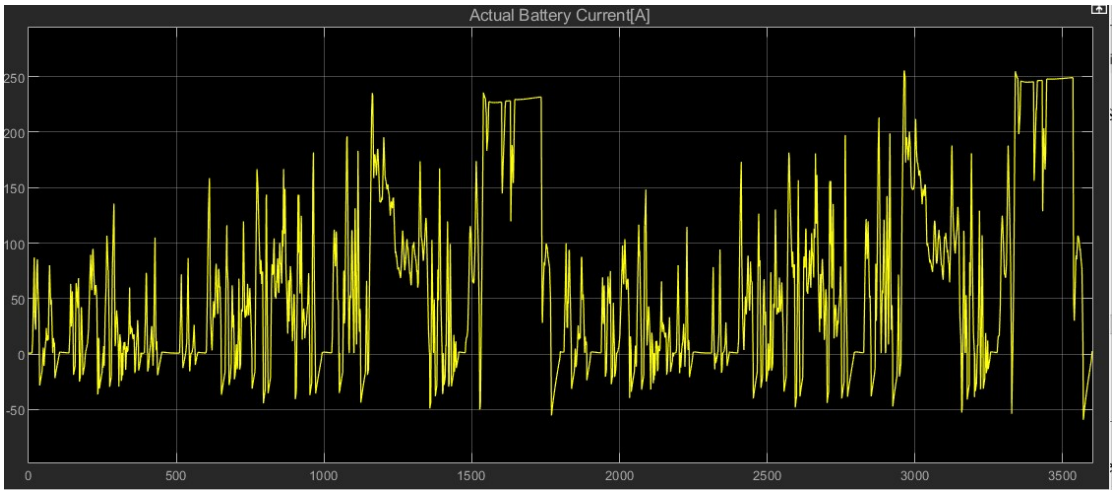

Figure 4-6 Battery Pack Output Current

By importing this current signal as an input signal into our EKF module, we can obtain our SOC monitoring results based on the WTP3 operating conditions

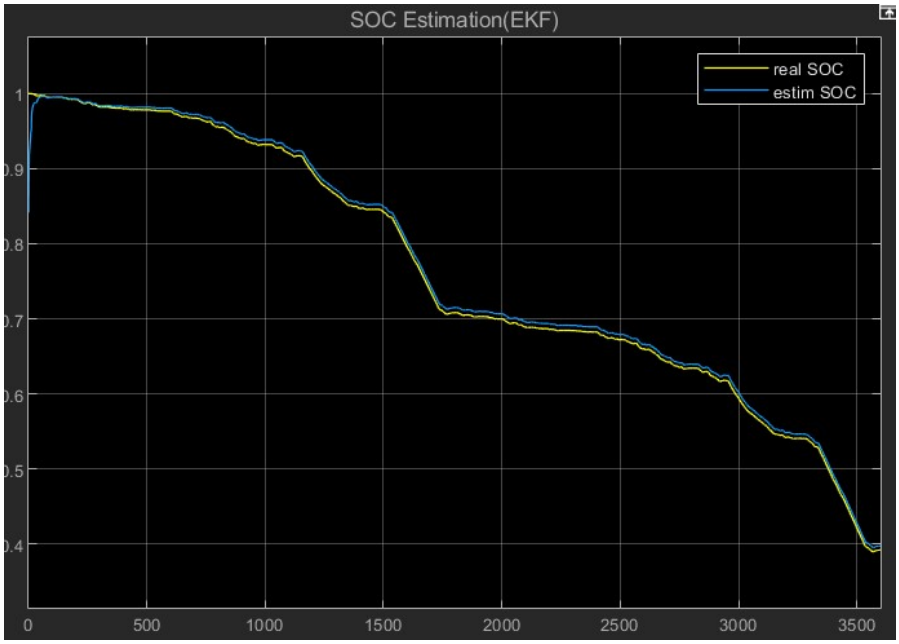

Figure 4-7 SOC Estimation Result

By observing the results, we find that the algorithm is able to fit the real-time SOC variation of the vehicle during travel relatively well. However, we also observed

the presence of errors in some of the variation cases. In this regard, the error image is shown in the following figure.

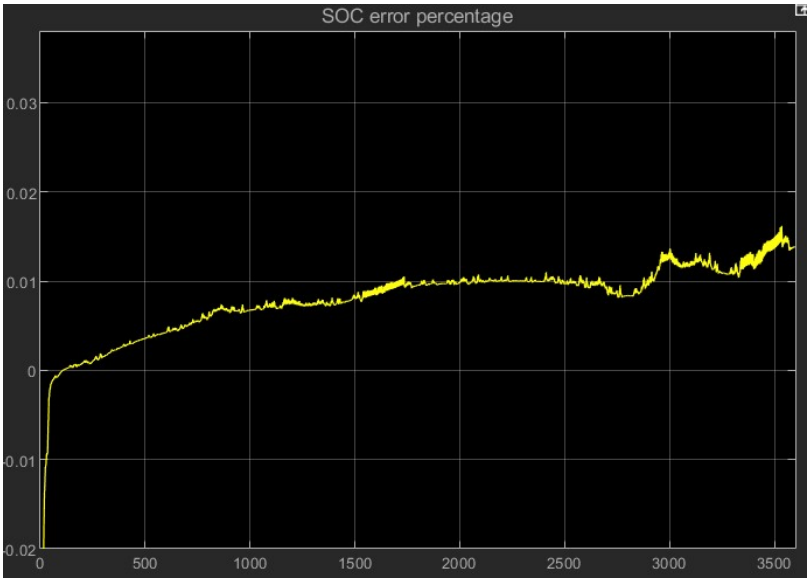

Figure 4-8 SOC error analysis

At this point, we can see that in the case of relatively large SOC, the error between our monitored SOC and the real SOC is still in a relatively small interval, and the whole monitoring error is less than two percent. In order to observe the situation when the battery is almost depleted, we perform a multi-cycle discharge process on the battery.

Figure 4-9 Continuous Discharge Image

We are able to see a large error in our observation mechanism when the SOC is less than 0.1.

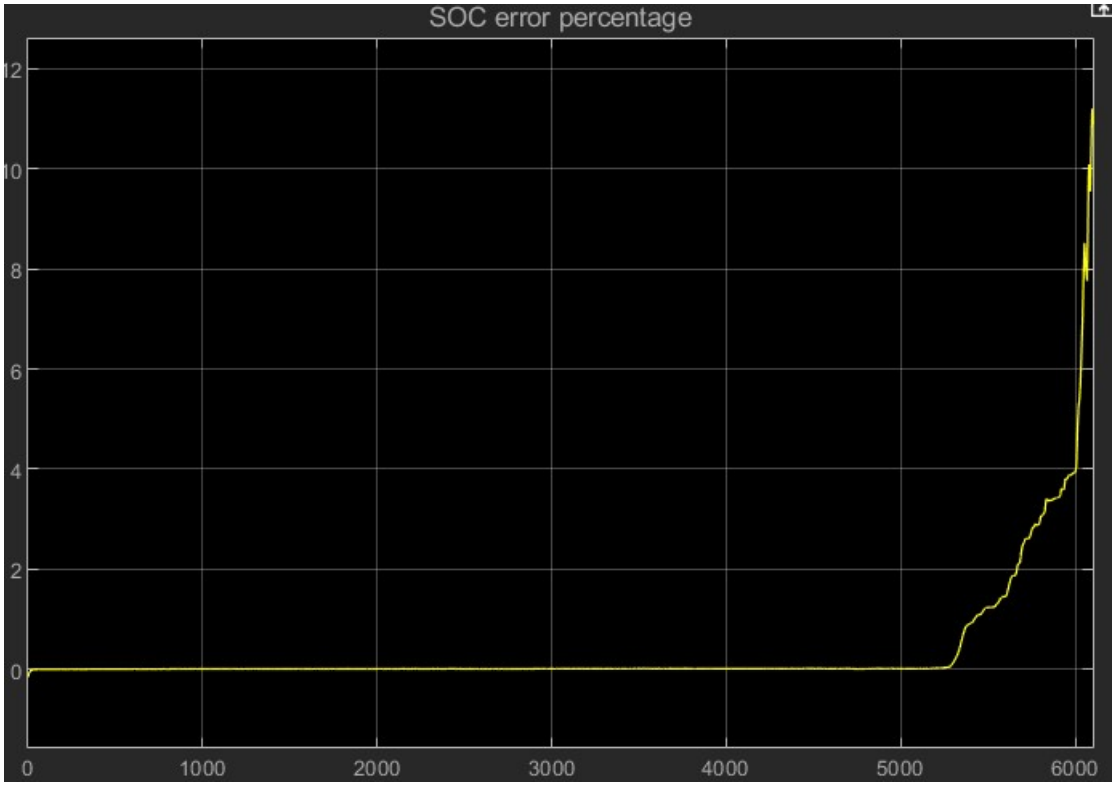

Figure 4-10 SOC error during continuous discharge

Note that in this image above, the straight line at the beginning does not represent a SOC error of 0, but is due to an axis scale issue. The error here is small enough to be considered as meeting the requirements of our observation. But what we see here is a very large error at SOC less than 0.1, with values of 12% or more.

It can be seen that the predicted SOC results based on the EKF algorithm fluctuate around the theoretical reference value of SOC, showing strong followability, and the maximum relative error does not exceed 0.02 throughout the experimental pulse current discharge condition, which is more accurate. This shows that the EKF algorithm can effectively predict the battery charge state even under complex current conditions.

But also here is due to the strong polarization nonlinearity of the battery at the end of discharge, when the battery model parameters change drastically with SOC, resulting in a rapid increase of the difference between the output voltage of the battery equivalent circuit model and the actual battery terminal voltage, thus showing a large prediction error. Therefore, the power battery should avoid working in the low SOC (0~0.1) range as much as possible in use.

4.1.3 SOH estimation through EKF

The SOH is an important indicator to evaluate the degradation of power battery performance as the user's use time grows. The aging of the battery shows a decrease in the total energy released and a reduction in output power externally, and a significant increase in the ohmic internal resistance internally, so the ohmic internal resistance of the battery under normal conditions can usually be used as a characterization of SOH.

The internal resistance can be obtained by applying a given excitation current to the battery and recording the voltage difference between the terminal voltages of the battery instantaneously to obtain the internal resistance of the battery according to Ohm's theorem; or by impedance measurement with the help of electrochemical workstation. However, most of these methods require separate off-line testing of the power battery, and in practice, it is often not desirable to shut down the power equipment for testing[29]. Therefore, in this paper, the internal resistance R0 of the battery is considered as a state value that changes continuously with the system, and the internal resistance parameter is estimated using the EKF algorithm.

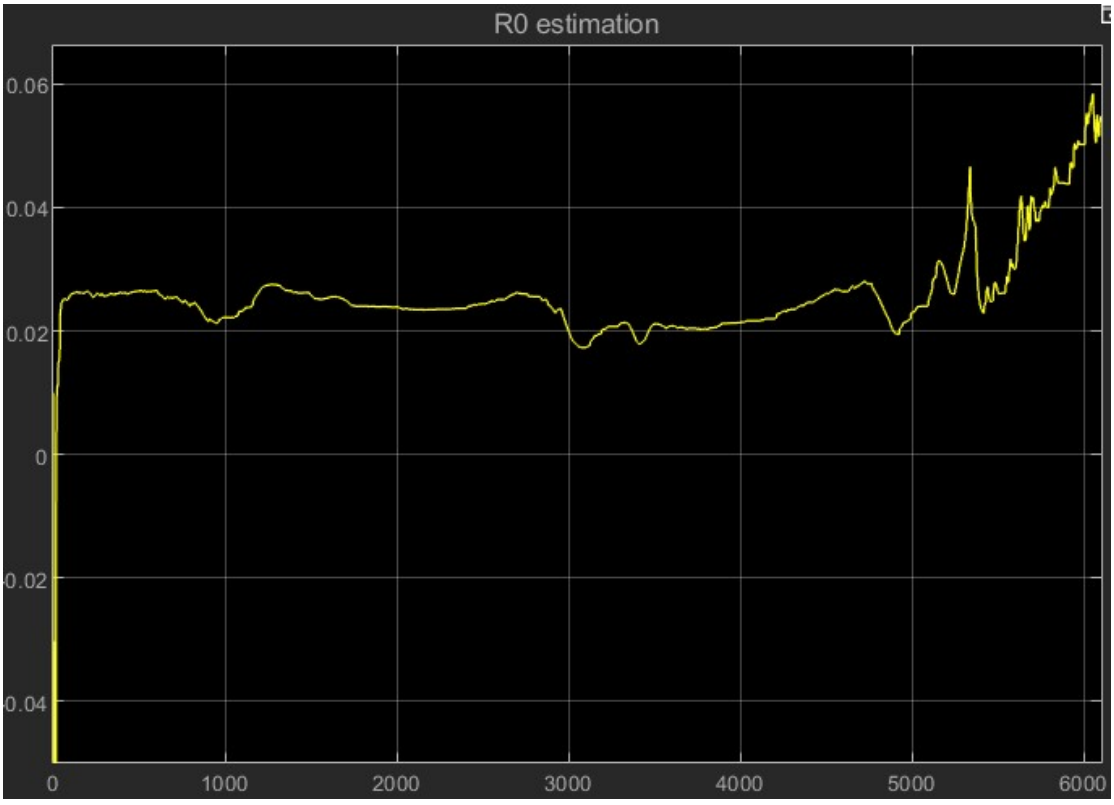

Figure 4-11 R_0 Estimation

When starting the algorithm to estimate the internal resistance of the battery, it can be found that the initial estimated internal resistance of the battery differs greatly from the reference value, but after the iterative calculation of the EKF algorithm, the predicted internal resistance quickly converges to fluctuate around the reference value, and the real-time internal resistance of the battery can be estimated more accurately. The simulation results also show that the EKF algorithm can effectively estimate the internal resistance of the battery.

At the same time we can also see that in the SOC less than 0.1 interval, the internal resistance of our battery pack increases sharply, which can also be reflected in the battery in the low SOC when power consumption is faster, the power is more unmanageable actual.

4.2 SOC estimation through UKF Algorithm

We now apply the UKF algorithm to the detection mechanism of the SOC in practice as well. The process is similar to the EKF, except that the results of the real-time simulation of the SOC will be slightly different due to the difference in algorithms.

4.2.1 Estimation of SOC logic diagram by UKF

The logic diagram of the UKF is basically the same as the EKF, here we choose to present it as an electrical diagram.

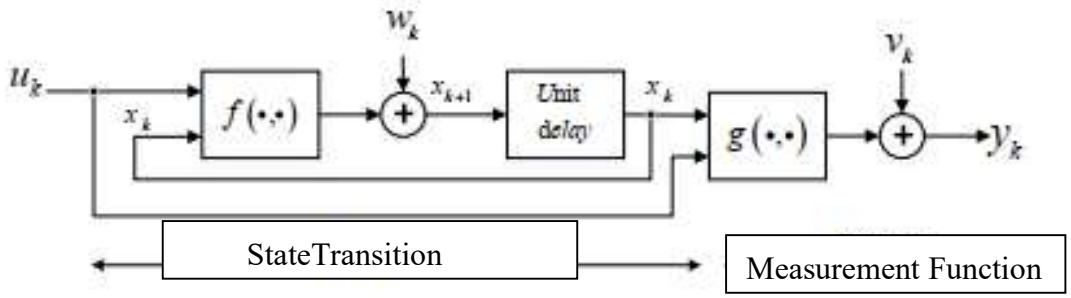

Figure 4-12 The logic diagram of the UKF

The covariance array of the system noise w_k, the covariance array of the system measurement noise v_k . These values are calculated in the equations in Chapter 3.

The input of the model is the terminal voltage and current data collected during the operation of the battery. In order to better compare the estimation effect, the test value of SOC is also used as input here, but it is not involved in the calculation.

The model consists of two parts, one is to implement the prediction process, i.e., to obtain the estimated value of the state variables SOC and Up from the optimal value of the state variables at the previous time through the state equation, and the implementation module is shown in Fig. The implementation module is shown in Fig. The SOC estimation model based on the UKF algorithm is calculated once for each set of input data to obtain the SOC estimation value at that moment[30].

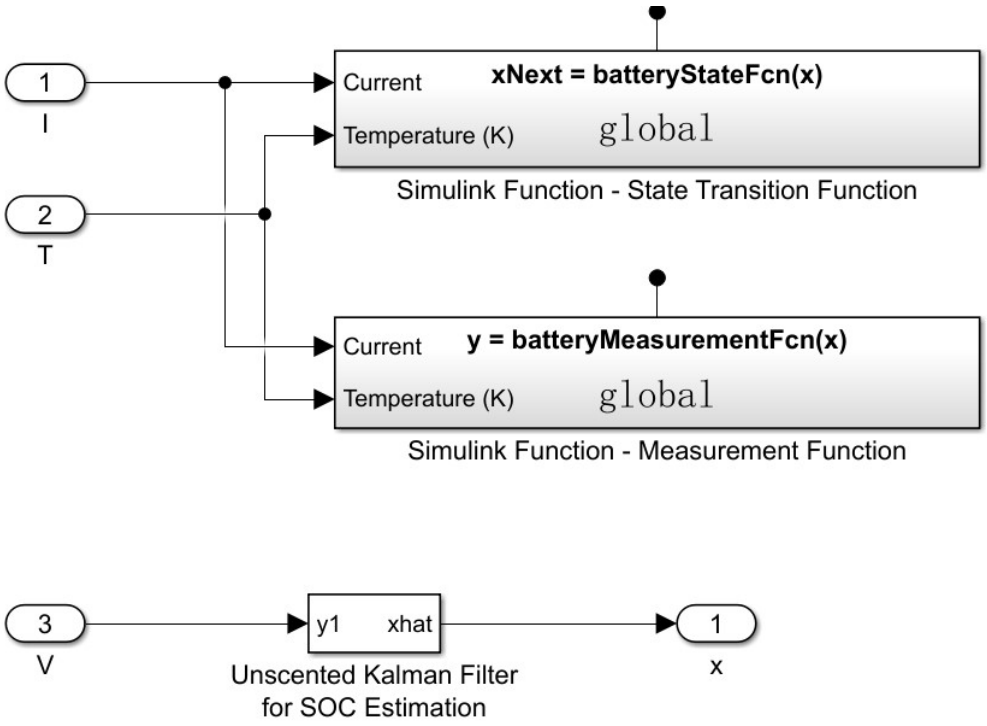

Figure 4-13 UKF-based top-level model for SOC estimation

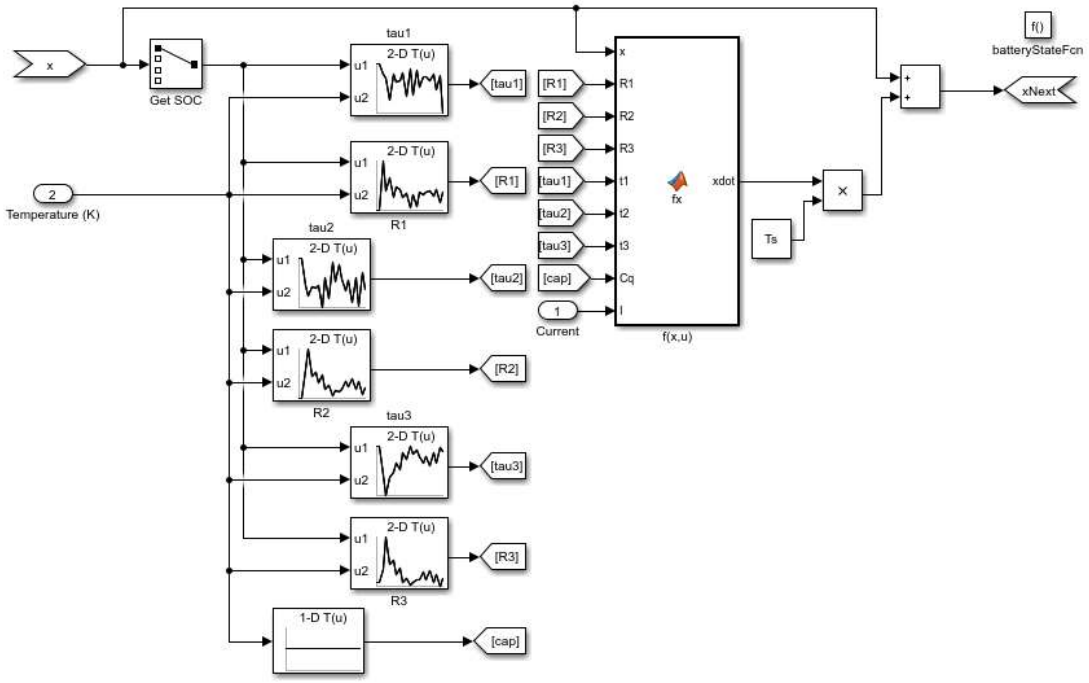

Figure 4-14 Simulink model for prediction module

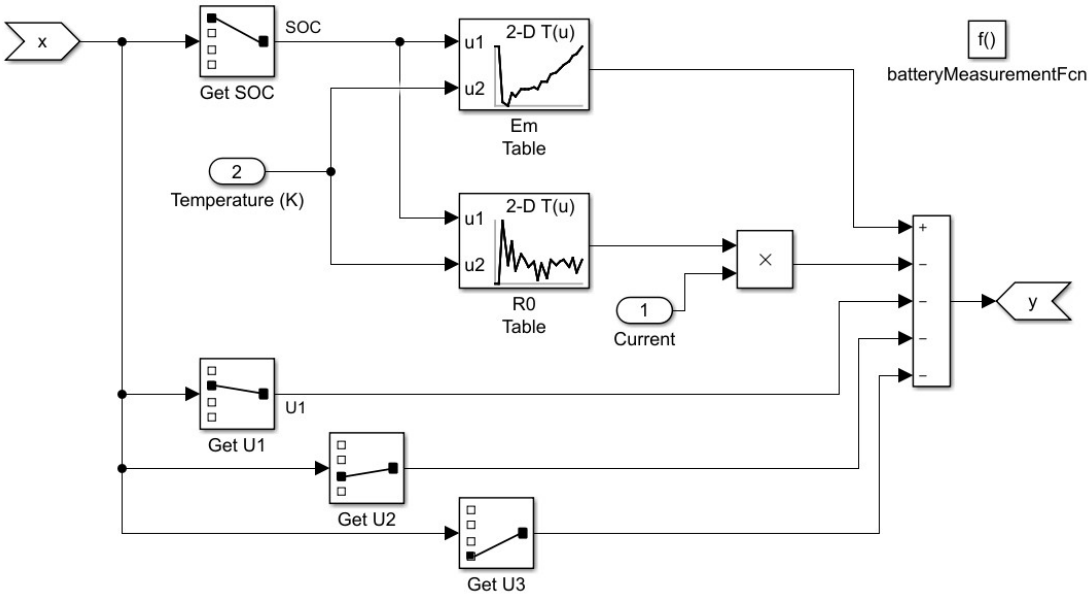

Figure 4-15 Updated Simulink model of the module

4.2.3 Monitor result

Similarly, here we set the initial value of SOC of our algorithm to 0.95 to observe the convergence rate of our algorithmic model. We can see that in a very short time, the SOC value calculated by the algorithm converges quickly to a value near the SOC value estimated by the ansatz integration method. This shows that our algorithm is more capable of coping with complex operating conditions. The specific observation results are shown in the following figure.

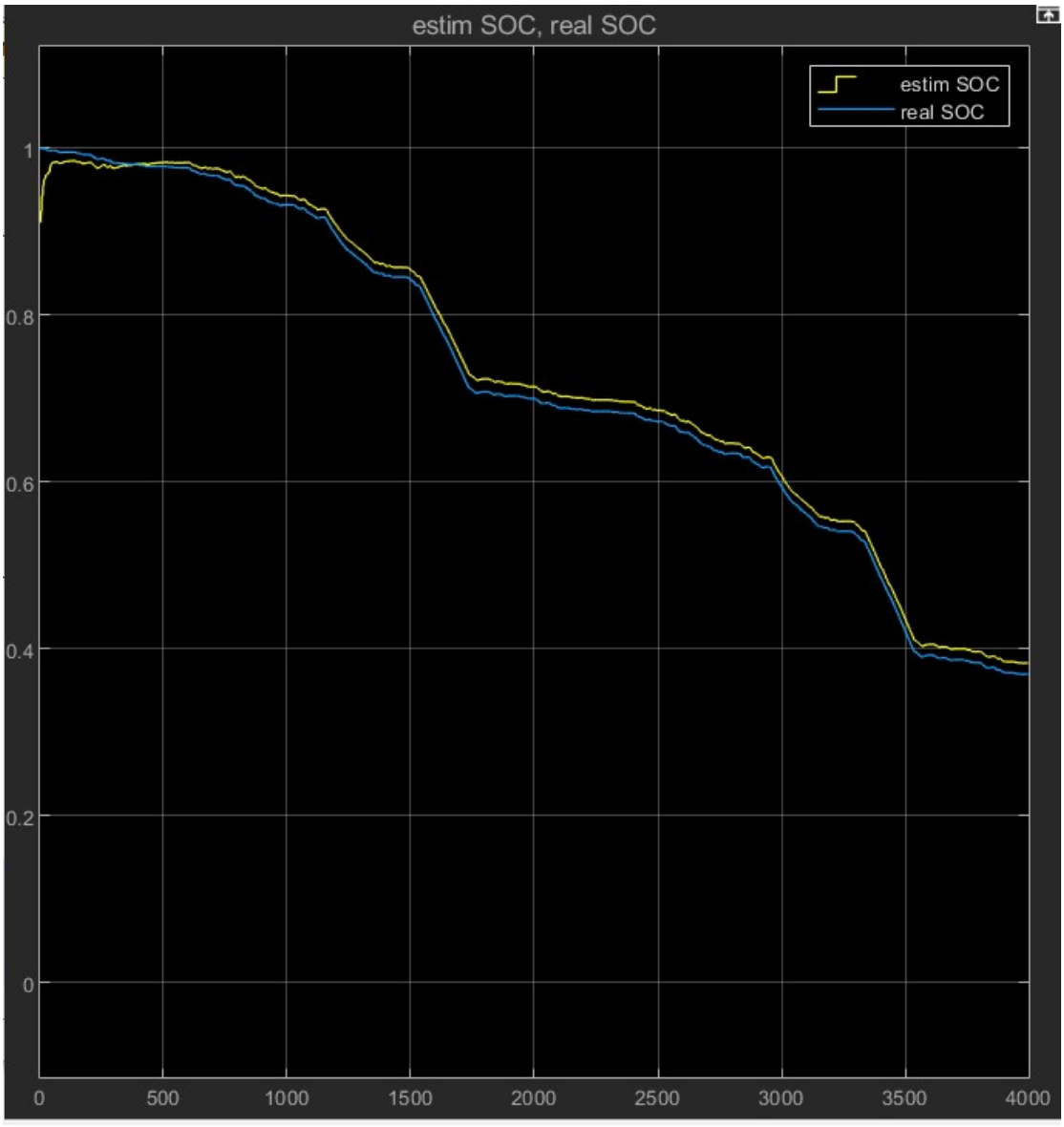

Figure 4-16 UKF-based SOC observation results

We are equally interested in the computational error of the UKF-based model. The figure below shows the results of the error calculation. We can see that the error of this model is somewhat larger compared to the EKF model. The error is close to 4 percent when the SOC value reaches 0.4. In fact, such a result can also be seen on the SOC plot. We can see clearly that the distance between the two lines is greater than the same EKF-based case.

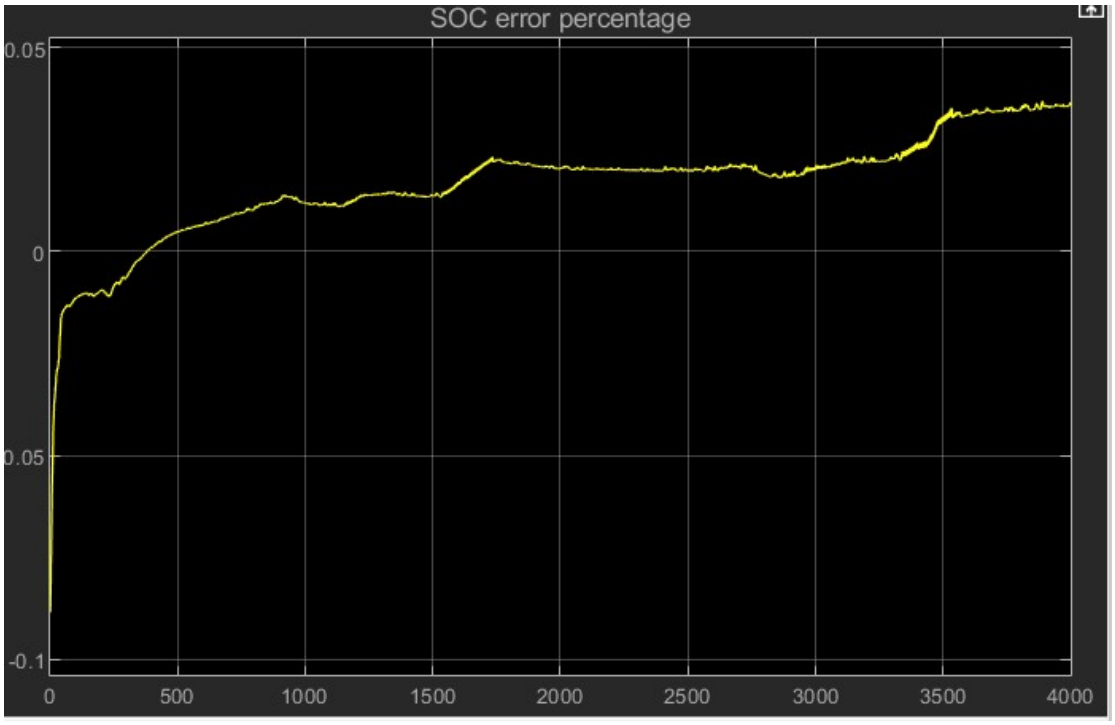

Figure 4-17 SOC error based on UKF

And by continuously discharging the battery under this model to a charge of 0, we can see the results as shown in Figure 4-18. Again, at SOC values less than 0.1, our estimates become inaccurate. And although the estimation error generated at this point is smaller than the error generated in the EKF algorithm, this error becomes smaller without much practical application.

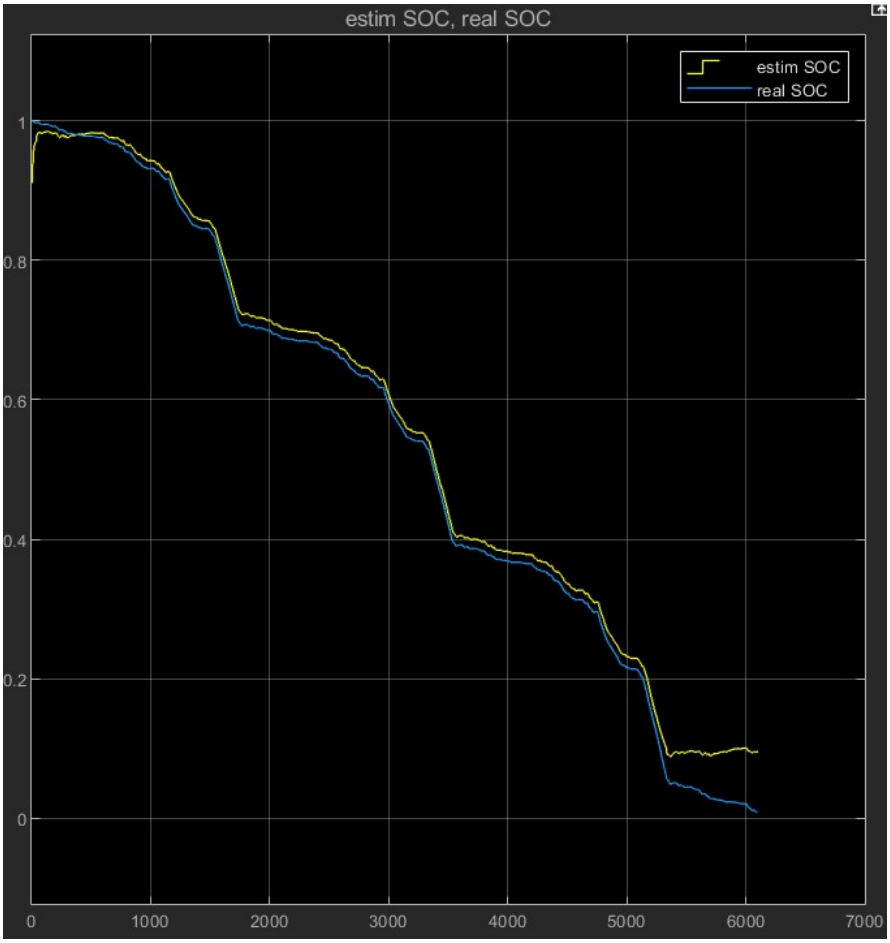

Figure 4-18 Calculated value of SOC discharged to 0 (based on UKF)

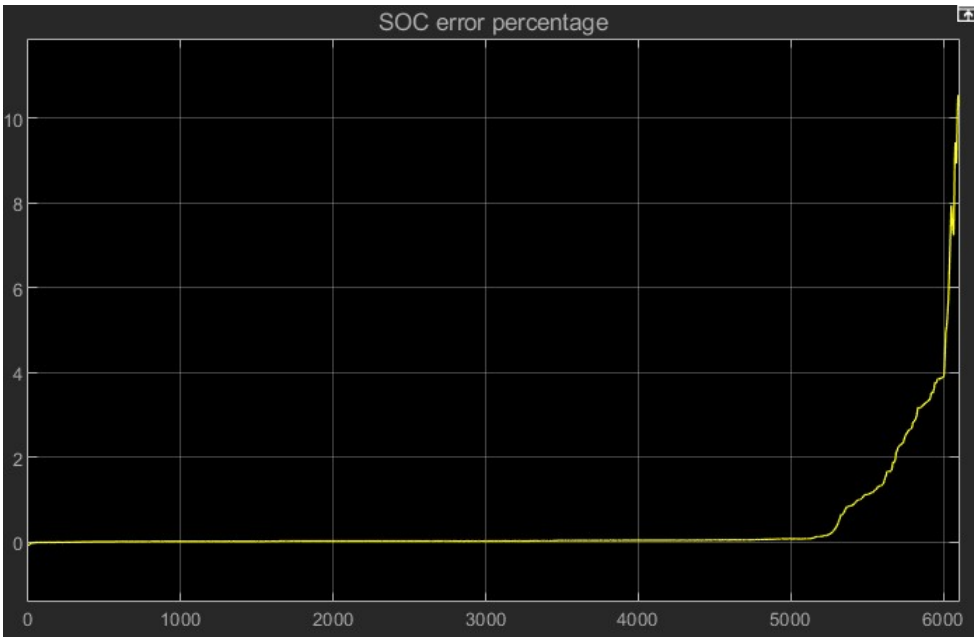

Figure 4-19 SOC error value for discharge to 0 (based on UKF)

4.3 Comparison of the accuracy of the two algorithms

Due to the obvious fluctuation of current in charging and discharging conditions, the change of battery SOC is non-linear (fluctuating) downward, and the SOC estimation curves of EKF and UKF can follow the reference curve of battery SOC more accurately and conform to the overall change of SOC. From the SOC estimation error in the figure, it can be seen that the EKF algorithm has a smaller SOC estimation error than the UKF algorithm under the same working condition. However, as the working condition continues, the error of SOC estimation by UKF increases gradually after 1000s, and the maximum error is 4%, and the maximum error of SOC estimation by EKF is 1.5%. Therefore, in this experiment, the EKF is more accurate than the UKF algorithm for SOC.

The model parameters in the UKF algorithm are: process noise and observation noise v, and their variances Q, R. Process noise is the error caused by the inaccuracy of the system model and the noise in the input quantities, in this paper it is caused by the inaccuracy of the cell model and the error in the measurement of the input current; observation noise is the error caused by the inaccuracy or interference in the measurement of the observed quantities, which in this paper refers to the errors caused by inaccurate or disturbed measurements of the terminal voltage[31]. Q and R have a significant impact on the accuracy of the algorithm, and it is assumed in the paper that both process noise and observation noise are Gaussian white noise, if R takes a larger value compared with Q, which means that the observation noise fluctuates more and the observation measurement accuracy is not high, at this time the prediction of the state equation plays a dominant role, and the estimation of SOC mainly depends on the prediction of the state equation, if R takes a smaller value compared with Q value is small, it means that the observation noise fluctuation is small and the accuracy of the observation is high, and the correction of the observation equation plays a dominant role at this time. The variance of the process noise and the observation noise as a fixed value, if too small will make the calculation results appear biased, if too large may make the results scattered.

The number of sigma points selected also has an impact, this paper is taken once. The sigma point is taken once, and the sigma point is taken twice. The difference between the two is that the UKF algorithm with one sigma point is to obtain the sigma point of the current moment from the optimal value of the previous moment, while the UKF algorithm with two sigma points is to obtain the sigma point of the middle moment from the optimal value of the previous moment, calculate the mean and variance of the middle moment from the sigma point of the middle moment, and then calculate the mean and variance of the current moment from this mean and variance.

The mean and the variance of the middle moment are used to calculate the sigma point of the current moment, and the subsequent calculation is exactly the same.

4.4 Summary of this chapter

The main content of this section is to establish a logic flow framework based on the EKF and UKF models respectively, and on this basis to establish the SIMULINK model for simulation. By integrating these two models into our EV simulation platform, we obtain real-time SOC and SOH (mainly the internal resistance R0) estimation results.

As can be seen from the images, both models converge quickly to near the exact SOC value in real time, while the maximum estimation error under general driving conditions does not exceed 4 percent. This indicates that our models can be used for the task of monitoring SOC and SOH in real time. However, at the same time, it can be seen that the UKF model performs relatively poorly, which the authors also analyze at the end of the paper as a result of the observation noise and the selection of sigma points.

CHAPTER 5

Full summary and outlook

5.1 Summary

In this paper, the SOC and SOH of the battery are estimated by using a 2p28s power pack of 50Ah from Samsung as the research object and a pure electric model of the classic car Panda as the carrier.

(1) The basic performance parameters of the battery are described, the basic characteristics of the battery under study are analyzed, and a series of curves of the basic characteristics of the battery are obtained. At the same time, the characteristic parameters of the battery during charging and discharging are analyzed, and the voltage and current performance of the battery during charging and discharging is profoundly demonstrated.

(2) After comparing several commonly used battery models, the Thevenin equivalent circuit model is chosen as the model for this paper, and the third-order RC battery model is modeled and the parameters of the Thevenin model are identified. In this paper, the lowest squares method is used to fit the parameters of the RC circuit. The fitted curves are finally fitted to achieve near agreement with the voltage signal generated from the pulsed current signal.

(3) The principle of Kalman filtering algorithm is introduced, the state equation and observation equation for the algorithm prediction are established, and the estimation process of the algorithm is described.

The UKF and EKF are applied to monitor the SOC and SOH of the vehicle power supply in real time during the travel process, respectively. The validity and accuracy of the two models are verified, and the prediction accuracy of the algorithm is improved. The less satisfactory experimental results are illustrated.

5.2 Future follow-up work

Based on this paper, the authors believe that the future can continue to improve and improve the work:

Temperature has a greater impact on the use of the battery process, the lower or higher the temperature, the battery capacity, internal resistance and self-discharge rate have a greater impact. In this paper, only the estimation accuracy of the battery model under a temperature condition is studied, and the temperature factor is not added to the algorithm prediction of the battery state, which is carried out under normal temperature conditions. In the subsequent research work, the temperature influence factor should be added to the algorithm research of battery state.

Many scholars have tried to use temperature correction coefficients, Arrhenius temperature acceleration model and electrochemical model to correct and estimate the battery model and state parameters, but there are still some uncertainties in the accuracy and reliability of the temperature correction model. The temperature of the system is changing with use at any time, and although the temperature parameters at the instant of sampling moment can be measured instantaneously, the question of what effect the temperature parameters have on the whole life cycle of the battery, what system states or parameters are caused to change and the design of the equivalent circuit model of the battery with temperature parameters will be the direction and focus of this area during future research.

On the basis of the thesis research, the online identification of battery model parameters can be extended to further improve the accuracy of the battery model output by using the battery external finite measurable to update the internal parameters of the model in real time through algorithmic calculation, because the battery parameters are also changing during use, which means that not only the earliest parameter estimation is also applicable in the subsequent. Implementing online identification of battery model parameters requires a large number of experiments as a basis, increased complexity of algorithms, and more efficient processors for computation

References

[1] Tobishima S, Yamaki J. A consideration of lithium cell safety[J]. Journal of Power Sources,1999, 81: 882-886

[2] Nagaura T. 4th international rechargeable battery seminar[J]. Deerfield Beach, FL, 1990

[3] Barsoukov, Evgenij, and J. Ross Macdonald, eds. Impedance spectroscopy: theory,experiment, and applications. Wiley-Interscience, 2005.

[4] Xin Zhe, Ge Yuanyue, Bo Wei, et al. Design of microcontroller-based battery management system for pure electric vehicle[J]. Nongye Gongcheng Xuebao/transactions of the Chinese Society of Agricultural Engineering, 2014, 30(12): 163-170

[5] Kaiya H, Ookawa T. Improvement in cycle life performance of high capacity nickel-metalhydride battery[J]. Journal of alloys and compounds, 1995, 231(1): 598-603

[6] MacLean G K, Aiken P A, Adams W A, et al. Preliminary evaluation of rechargeablelithium-ion cells for an implantable battery pack[J]. Journal of power sources, 1995, 56(1):69-74.

[7] Wenzl H, Baring-Gould I, Kaiser R, et al. Life prediction of batteries for selecting thetechnically most suitable and cost effective battery[J]. Journal of power sources, 2005, 144(2):373-384.

[8] Lin C H, Wang C M, Ho C Y. Implementation of state-of-charge and stateof-health estimation for lithium-ion batteries[C]//IECON 42nd Annual Conference of the IEEE Industrial Electronics Society. Florence: IEEE Press, 2016:4790-4795.

[9] Wei Jingwen, Dong Guangzhong, Chen Zonghai. Remaining useful life prediction and state of health diagnosis for Lithium-ion batteries using particle filter and support vector regression[J]. IEEE Transactions on Industrial Electronics, 2018, 25(7): 5634-5643.

[10] Qin Taichun, Zeng Shengkui, Guo Jianbin. Robust prognostics for state of health estimation of lithium-ion batteries based on an improved PSO–SVR model[J]. Microelectronics Reliability, 2015, 55(9-10): 1280-1284.

[11] Hung M H, Lin C H, Lee L C, et al. State-of-charge and state-of-health estimation for lithium-ion batteries based on dynamic impedance technique[J]. Journal of Power Sources, 2014, 28(4): 861-873

[12] Yang Zhang, Bo Guo. Online capacity estimation of Lithium-ion batteries based on novel feature extraction and adaptive Multi-Kernel relevance vector machine[J]. Energies, 2015, 8(11): 12439-12457

[13] wuzhao Yan, Bin Zhang, Guangquan Zhao, et al. Battery management system with lebesgue sampling-based extended kalman filter[J]. IEEE Transactionson Industrial Electronics, 2019, 36(4): 3227-3236.

[14] Arijit G, Amit P. State of health estimation of lithium-ion batteries using capacity fade and internal resistance growth models[J]. IEEE Transactions on Transportation Electrification, 2018, 4(01): 135-146.

[15] Spotnitz R. Simulation of capacity fade in lithium-ion batteries[J]. Journal of power sources,2003, 113(1): 72-80.

[16] Widodo A, Shim M C, Caesarendra W, et al. Intelligent prognostics for battery healthmonitoring based on sample entropy[J]. Expert Systems with Applications, 2011, 38(9):11763-11769.

[17] Liu X T, Qin S X, He Y, et al. SOC estimation of the lithium-ion batterywith the temperature-based Nernst model[C]//Power Electronics & Motion Control Conference. Hefei: IEEE Press, 2016: 1419-1422.

[18] Ping Shen, Ouyang Minggao, Lu Languang, et al. The co-estimation of stateof charge, state of health and state of function for Lithium-ion batteries in electric vehicles[J]. IEEE Transactions on Vehicular Technology, 2018, 67(01):92-103.

[19] Huachun Han, Haiping Xu, Zengquan Yuan, et al. A new SOH prediction model for lithium-ion battery for electric vehicles[C]//2014 17th International Conference on Electrical Machines and Systems (ICEMS). Hangzhou: IEEE Press, 2014: 997-1002.

[20] Cannarella J, Arnold C B. State of health and charge measurements in lithium-ion batteries using mechanical stress[J]. Journal of Power Sources, 2014, 29(2): 7-14.

[21] Huan Li, Ravey A, N'Diaye A, et al. State of health estimation of lithium-ion batteries under variable load profile[C]//Conference of the IEEE IndustrialElectronics Society. Beijing: IEEE Press, 2017: 5287-5291

[22] Kim J, Cho B H. State-of-charge estimation and state-of-health prediction of a Li-Iondegraded battery based on an EKF combined with a per-unit system[J]. VehicularTechnology, IEEE Transactions on, 2011, 60(9): 4249-4260.

[23] Andre D, Appel C, Soczka-Guth T, et al. Advanced Mathematical Methods of SOC and SOHEstimation for Lithium-Ion Batteries[J]. Journal of Power Sources, 2012

[24] Kim J, Lee S, Cho B H. Complementary cooperation algorithm based on DEKF combinedwith pattern recognition for SOC/capacity estimation and SOH prediction[J]. PowerElectronics, IEEE Transactions on, 2012, 27(1): 436-451.

[25] Chun C Y, Seo G, Cho B, et al. A fast state-of-charge estimation algorithm for LiFePO 4batteries utilizing extended Kalman filter[C]. //ECCE Asia Downunder (ECCE Asia), 2013IEEE. IEEE, 2013:912 - 916.

[26] atteo Galeotti, Corrado Giammanco, Lucio Cinà, et al. Synthetic methods for theevaluation of the State of Health (SOH) of nickel-metal hydride (NiMH) batteries[J]. EnergyConversion and Management, 2015, 92:1-9.

[27] G.L.Plett. High-performance battery-pack power estimation using a dynamic cellmodel[J]. IEEE Transactions on Vehicular Technology, 2004, 53(5):1586-1593

[28] Adnan Nuhic, Tarik Terzimehic, Thomas Soczka-Guth, et al. Health diagnosis andremaining useful life prognostics of lithium-ion batteries using data-driven methods[J].Journal of Power Sources, 2013, 239:680-688

[29] JavierGazzarri(2021). BatteryModeling (https://www.mathworks.com/matlabcentral/fileexchange/36019-battery-modeling), MATLAB Central File Exchange. Retrieved March 16, 2021.

[30] FerahtiaSidali(2021). Batterymodel (https://www.mathworks.com/matlabcentral/fileexchange/82385-battery-model), MATLAB Central File Exchange. Retrieved March 25, 2021.

[31] Pei Lei, Zhu Chunbo, Wang Tiansi, et al. Online peak power prediction based on aparameter and state estimator for lithium-ion batteries in electric vehicles[J]. Energy, 2014,66:766-778.

Appendix

Full view of SIMULINK model